Climate change increases heat-health risks from 2026’s May and June heatwaves

Authors

Clair Barnes, *Centre for Environmental Policy, Imperial College, London, UK*
Ben Clarke, *Centre for Environmental Policy, Imperial College, London, UK*
Claire Bergin, *ICARUS Climate Research Centre, Maynooth University, Maynooth, Ireland*
Mark McCarthy, *Met Office,* Exeter, UK
Fraser Lott, *Met Office,* Exeter, UK
Mariam Zachariah, *Centre for Environmental Policy, Imperial College, London, UK*
Theodore Keeping, *Centre for Environmental Policy, Imperial College, London, UK*
Garyfallos Konstantinoudis, *Grantham Institute for Climate Change and the Environment, Imperial College, London, UK*
Archie Rayner, *School of Public Health, Imperial College, London, UK*
Malcolm Mistry, *Environment & Health Modelling Lab, London School of Hygiene and Tropical Medicine, London, UK*
Antonio Gasparrini, *Environment & Health Modelling Lab, London School of Hygiene and Tropical Medicine, London, UK*
Friederike Otto, *Centre for Environmental Policy, Imperial College, London, UK*

Review authors

Emmanuel Raju, *Copenhagen Center for Disaster Research, Department of Public Health*, University of Copenhagen
Emily Theokritoff, *Grantham Institute for Climate Change and the Environment, Imperial College, London, UK*
Ross Thompson, *UK Health Security Agency, London, UK*

Main findings

- During the 2026 May and June heatwaves, early estimates suggest that as many as 2700 people could have died across the UK as a result of the heat, with just under half of those due to the additional heat added by human-induced climate change. We estimate a total of 553 (95% empirical Confidence Intervals: 426 - 704) excess heat-related deaths during 21-29 May 2026 and 2,183 (95%eCI: 1,582 - 2,724) during 18-28 June 2026 in England and Wales.
- Out of the 553 estimated heat-related excess deaths in May, we found that 327 (95% eCI: 191 - 461) can be attributed to human induced climate change, whereas out of the 2,183 in June 825 (95% eCI: 441 - 1,230) can be attributed to human induced climate change. This corresponds to 59% in May (95% eCI: 36 - 75%) and 38% in June (95% eCI: 22 - 53%). The lower proportion during the June heatwave reflects the extremeness of the temperatures, which would have resulted in very high heat-related excess mortality even without the additional contribution from human-caused warming.
- The two heatwaves in May and June were extreme, even in today's climate. Both heatwaves affected a very large area and set new records across England and Wales as a whole, with the highest temperatures ever recorded for May (35.1°C at Kew Gardens, London on 26 May) and on three consecutive days in June, with temperatures provisionally exceeding 37°C at several stations in East Anglia, each breaking the previous record by over 1.5°C.
- The May heatwave was particularly intense across southern and southeastern England, while the June heatwave was most exceptional across southern and southwestern England, with local return periods for the time of year in some counties exceeding 200 years. However, estimates of excess mortality associated with the extreme heat per million inhabitants suggest that the impact of the high temperatures was equally severe in the Midlands and the south-west (even for the May event), which are less frequently exposed to such extreme heat than London and the south-east.
- Such high temperatures over an area this large are unusual even at the height of summer in July and August: similarly extreme heat over the whole of England and Wales would be expected to occur around once every twenty years in the current climate. Human-induced climate change has substantially increased the intensity of these events. In a climate without human-caused warming, the maximum temperatures would have been much less likely to occur and would have been around 3-4°C cooler.
- We note that of the 1.4°C of global warming that humans have caused to date, around 1.1°C has occurred since 1976, when the previous June temperature record was set. We estimate that peak UK temperatures are now around 2-3°C hotter than they would have been in 1976.
- The change in the likelihood of such an intense period of nighttime temperatures is even more striking. Across all datasets, we find that nighttime temperatures of this

intensity would have been essentially impossible in a world without human-caused warming.

- In climate model simulations, human-caused warming due to greenhouse gases is estimated to have made such heatwaves 3 to 7 times more likely to occur and 1.4°C to 1.8°C more intense; the climate model assessment is based on changes up to the recent past, rather than up to 2026, so we consider this to be a conservative estimate.
- The June heatwave was particularly unusual in terms of the high humidity, reflected in exceptionally high Wet Bulb Globe Temperature (WBGT) values. Humid heat is more dangerous than dry heat because it impairs the body's ability to cool itself by sweating. Compared with a preindustrial climate, 3day-maximum WBGT during the June event was around 3°C higher.
- These record-breaking heatwaves, and the associated expected excess deaths, highlight the urgent need for heat adaptation and preparedness, alongside mitigation efforts to cut emissions and halt further warming. Closer attention must be paid to heat risk governance, with a focus on heat action plans. The future possibility of similarly unprecedented heatwave events must be considered in long-term adaptation planning, ensuring adequacy and effectiveness of measures, especially to protect the most vulnerable and exposed members of society.

Introduction

By the end of June 2026, Europe had already experienced two record-breaking heatwaves. First, in the midst of the world's second hottest May on record (second only to May 2024; Reuters, 2026) Europe saw a 'mind-bogglingly crazy' early heatwave during the final week of the month. Temperatures began to rise across Europe on the weekend of the 24 and 25 of May as a 'heat dome' settled over western and central Europe (Severe Weather Europe, 2026). A heat dome in Europe is characterised by a persistent high-pressure system that draws warm air from Northern Africa into Western and Central Europe while blocking low-pressure systems from entering the area under the heat dome, allowing heat to build up. Temperature records for May were broken across Europe with 35.1°C recorded in Greater London, England, 32.9°C in Wales and 30.6°C in Ireland (UK Met Office, 2026a, Met Éireann, 2026). Portugal broke its previous May record with 40.3°C recorded (The Portugal News, 2026) and France, Spain, Germany, and Switzerland also experienced dangerously high temperatures very early in the season. As the heat dome pushed north from Sunday 24th May (Figure 1.1), this caused more northern regions to experience significant heat disruption with amber health warnings being issued for significant parts of the UK (The Guardian, 2026). Both the UK and Ireland saw previous May records broken by in excess of 2°C (UK Met Office, 2026a, Met Éireann, 2026).

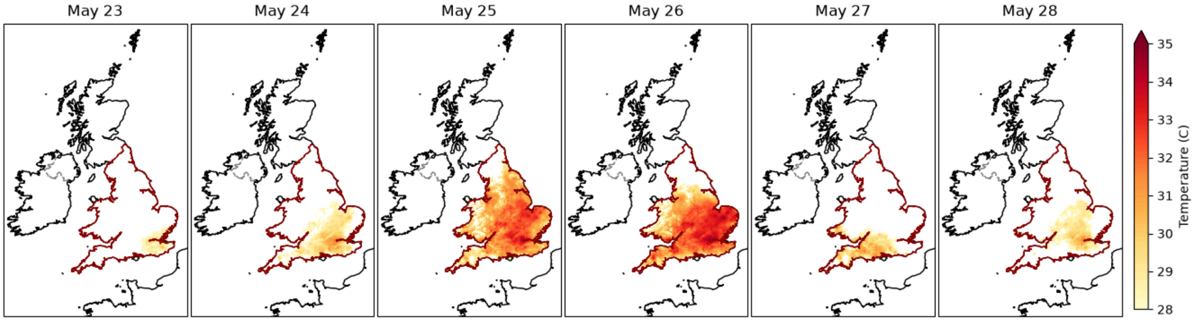

Figure 1: *Daily maximum temperatures exceeding 28°C from May 23rd-28th 2026. Data: HadUK-Grid (provisional).*

From the 18th of June 2026 onwards, Western Europe again experienced exceptionally high temperatures due to another persistent high-pressure system affecting large parts of the continent (Figure 1.2). In France, red heat alerts were issued across more than half of the country's departments, impacting an estimated 39 million people. More than 1,350 schools were closed (Guardian, 2026). Rare red warnings were issued across parts of the UK for three successive days. National records for both daytime and night-time temperatures were broken across the UK (Met Office, 2026), and multiple stations in East Anglia provisionally recorded temperatures above 37°C on 26 June, each surpassing the previous June record of 35.6°C (set in 1976) by over 1.5°C. The temperatures were accompanied by high humidity and unusually warm overnight conditions, limiting opportunities for relief and increasing health risks for vulnerable groups (Guardian, 2026). In the Netherlands, the Royal Netherlands Meteorological Institute (KNMI) issued a Code Red weather warning, indicating a high likelihood of dangerous weather conditions in the southern and central parts of the country from June 24th through to June 27th with temperatures rising to 39.4°C (KNMI, 2026).

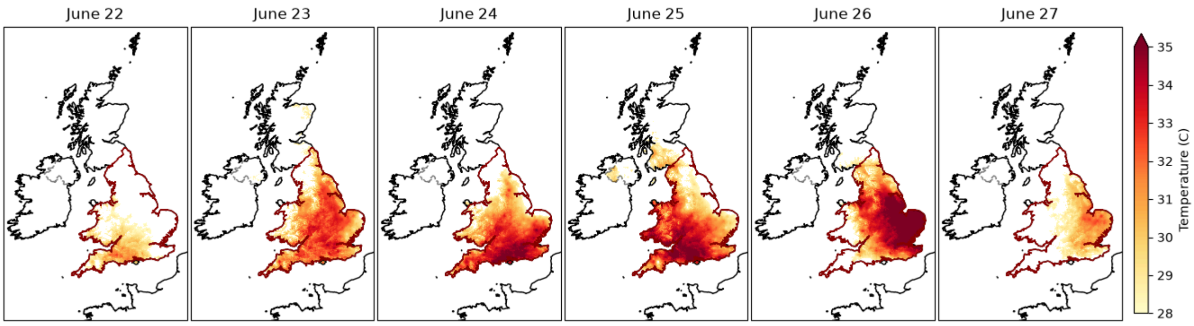

Figure 1.2: *Daily maximum temperatures exceeding 28°C from June 22nd-27th 2026. Data: HadUK-Grid (provisional).*

In this report we use established attribution and heat risk modelling methods to estimate the number of heat-related excess deaths across England and Wales during the two heatwaves, and also the proportion of those excess deaths that would have been avoided in a world without human-caused warming.

Health risks of extreme heat

As temperatures rise globally, the European Environment Agency (EEA) describes heat as "the largest and most urgent climate hazard for human health" (EEA, 2024), while the WHO recently called for authorities in Europe to plan for extreme heat as they would for winter flu (WHO, 2026). A global study focusing on heatwaves in 2023 showed that more than half (54.29%) of the 178,000 heat-related excess deaths were due to human-caused climate change (Hundessa et al., 2025). In general, tens of thousands of excess heat-related deaths occur across Europe each year (Masselot, et. al., 2023; Ballester et al., 2023). Barnes et al., (2025) explored heat deaths in 854 European cities during the summer of 2025 and found that nearly 16,500 excess deaths could be attributed to climate change, with almost 70% of those attributable to human-caused warming. The UKHSA heat mortality monitoring report estimated 1,504 (95% CI: 936 to 2,072) deaths associated with 5 heat episodes during the summer of 2025 (UKHSA, 2026).

Population age and socio-economic factors are the main drivers that determine vulnerability to impacts from high temperatures (Falchetta et al., 2024), In the UK, women, ethnic minorities, people in older age groups and those living in the most deprived areas have an increased risk of deaths during periods of heat (Thompson et al., 2025). Many other vulnerable groups - such as unhoused populations and people living in prisons - also often do not receive sufficient consideration during extreme weather events. With Europe's population expected to age considerably over the coming decades (Eurostat, 2023), and temperatures rising particularly quickly in Europe (Copernicus, 2024), the collective risk from extreme weather events is expected to increase significantly in the future (Harrington and Otto, 2023; European Commission, 2025). While there is quantitative evidence that adaptation to extreme heat is taking place to a certain extent in some places (Vicedo-Cabrera et al., 2018, Stuart-Smith et al., 2025), large adaptation gaps still prevail and future impacts, including deaths from extreme heat, can still be avoided.

UK urban populations are growing (UK Government Office for Science, 2021). With urbanisation becoming more and more prevalent in Europe, cities are becoming hotspots of increased heat risk caused by the urban heat island effect, rapidly ageing populations, and urban growth pressures (World Bank, 2025; European Commission, 2025a). Currently, 75% of the population of the European Union lives in cities (World Bank, 2024), with more than 80% expected by 2050 (European Commission, 2020). Current mitigation policies in place around the world are projected to result in about 2.8°C warming above pre-industrial levels by 2100 (UNEP Emission Gap report, 2026), which would result in many more heat-related deaths and impacts globally. Extreme heat causes more than just deaths: it increases hospitalisations and worsens chronic illnesses, especially for older adults and low-income communities (World Bank, 2025). Heat stress also affects the UK labour force; survey results for the summer of 2024 suggest that a 1°C positive temperature anomaly from the long-term average increased the probability of a worker reducing their hours by 9.9% and their effort by 9.5% (Robinson et al., 2025). Jobs in outdoor environments, including construction, transport and tourism are particularly at risk (World Bank, 2025), while persistent heat also affects water availability and crop yields, which can have a spiralling effect on food shortage and inflation, as well as increasing the risk of wildfires.

Early season extreme heat feels particularly pronounced as people's bodies have not had the time to adjust to increased heat (UK Met Office, 2026b). Spring (March, April and May) is the fastest-warming season in the UK, suggesting that extreme early season temperatures will occur with increasing frequency in the future (Royal Meteorological Society, 2025). In May 2026 the UK's Climate Change Committee published its fourth independent assessment of UK climate risk (CCC, 2026), highlighting that the UK has been built for a climate that doesn't exist anymore and is not adapted to the needs of current and future climate change impacts. The top climate risk to be addressed is intensifying heat, with the report's recommended top adaptation target that "by 2050, excess heat-related mortality should be no greater, and ideally lower, than today's annual average." As the UK prepares the publication of its fourth National Adaptation Programme (due in 2028) and an increasing number of city level heat plans are formulated, such as Heat Ready London (Mayor of London, 2026), it is key to consider these wide-ranging and rapidly increasing risks to ensure that adaptation measures will be effective in the long-term. While science-based adaptation can be effective at reducing impacts, with increasing warming, limits to adaptation will increasingly be reached as more extreme temperatures are reached, underscoring the importance of pursuing mitigation and adaptation in parallel.

Changes in extreme heat in the UK

The latest state of the UK climate report found that the UK has been warming at a rate of approximately 0.25°C per decade, with recent heat episodes in central England exceeding any observed temperatures in at least 300 years (Kendon et al., 2025). The report also found that the number of days in the most recent decade considered (2015–2024) with temperature anomalies exceeding the 1961–1990 average by 5°C has doubled. In general over the UK, warm spells have more than doubled in length, going from 5.3 days between 1961 and 1990, to 13.2 days between 2008 and 2017 (UK Met Office, 2026c). The most significant changes were seen in southeast England, with the mean length of warm spells increasing from around 6 days to over 18 days per year over the same time periods. While one of the recent heat events studied here occurred in late meteorological spring and not summer, there is a clear climate change trend of increased record temperatures and sustained heatwaves occurring during UK summertime (Kay et al., 2025).

Previous attribution analysis shows that this rising occurrence of intense heat is unequivocally due to human-induced climate change, in the UK, across Europe and globally, though temperatures across Europe are known to have increased more than twice as much as the global mean (Copernicus, 2025), with a number of studies demonstrating high confidence that human-caused climate change is the primary contributor to these rising European temperatures (Seneviratne et al., 2021; Quilcaille et el., 2025). The first extreme event attribution study was on the hot European summer of 2003, finding that human-induced warming made such a hot summer more than twice as likely (Stott et al., 2004). Since then, numerous major heat events have elicited attribution studies (e.g. Christidis et al., 2015; Vautard et al., 2020; Leach et al., 2020; Zachariah et al., 2022; Feser et al., 2024; Ionita et al., 2024; Barnes et al., 2025; Bergin et al., 2026; Keeping et al., 2026). Consistently, such studies have found that heat extremes in Europe are warming at a rate much larger than the rate of global warming, and that the recent extreme events would have been very unlikely or virtually impossible without this warming. In the UK specifically, previous heat events have seen their likelihood and intensity directly linked to, and increased by, anthropogenic climate change (Zachariah et al., 2022 and Clarke et al., 2026), with intensity rising at a rate far beyond that of the global mean.

Given the dangers and costs posed by extreme heat, it is essential to understand how human-induced climate change is driving changes in severe and record-breaking events as they continue to occur and the implications of these changes. While attribution studies on heat events for the UK already exist, as described above, more granular information and greater sensitivity analysis is required to support effective adaptation planning.. This includes assessing different heat indices from maximum and minimum temperatures to humid heat metrics, doing so across different regions and spatial scales, and finally how these changes lead to impacts on people's health.

Study aims & scope

The first section of this report uses an established extreme event attribution methodology to analyse changes in extreme temperatures over England and Wales, and the extent to which those changes can be attributed to human-caused warming. We use this attributable change in intensity to estimate how much cooler the heatwaves would have been in a world without anthropogenic climate change, which would be around 1.4°C cooler than 2026 (Forster et al., 2026). This allows us to understand how unusual the temperatures reached during early summer 2026 were, both within the context of previous annual maxima and within the context of expected temperatures during May and June. We also report changes in the most extreme temperatures since 1976, when the previous June record was set. We focus on England and Wales because this captures the extent of the most extreme temperatures (see Figures 1.1 and 1.2), although temperatures in Scotland and Northern Ireland are also considered in Section 1.1.

In the second part of the report, we use established exposure-response relationships (Gasparrini et al., 2022) to estimate the excess mortality attributed to heat given the observed temperatures and also under the counterfactual scenario of a 1.4°C cooler world without human-induced climate change. By comparing these estimates, we calculate how many more people are expected to have died in each lower super output area (LSOA; 1,000 to 3,000 residents) during the early summer heatwaves in 2026 due to the excess heat caused by anthropogenic warming. We also report the expected proportion of heat-related deaths attributed to human-induced climate change.

1 Analysis of changing UK temperatures

1.1 Early summer 2026

Figure 1.3a shows the 3-day mean of daily maximum temperatures from May 24-26 in each county. The highest temperatures occurred across southern England, with daily maximum temperatures in Greater London and the surrounding counties reaching an average of around 32°C over the period. We use a statistical model fitted to the time series of annual and monthly maximum temperatures in each county to assess how unusual such high temperatures are across the UK. The rarity of an event is expressed as a 'return period' - how frequently, on average, we would expect to experience a similar or even more extreme event in today's climate. These estimates use the HadUK-Grid dataset (see Section 3.1.1), which interpolates station-based data from 1931 to June 2026 onto a 1km grid; any return period exceeding 100 years therefore indicates the most extreme event in the record. Return periods of 100 years or above should not be interpreted as a precise quantification of the 'true' likelihood of similar temperatures, but as a clear indication of very extreme temperatures.

Similar temperatures are relatively common across England and Wales in the height of summer, with return periods of ten years or less, but were somewhat more unusual for Scotland (panel b). However, similar temperatures are extremely unusual for May, with return periods well in excess of 100 years across England and Wales, with the most unusual temperatures occurring in the east and southwest of England (panel c). Night-time temperatures during the May heatwave were less unusual and are not shown here.

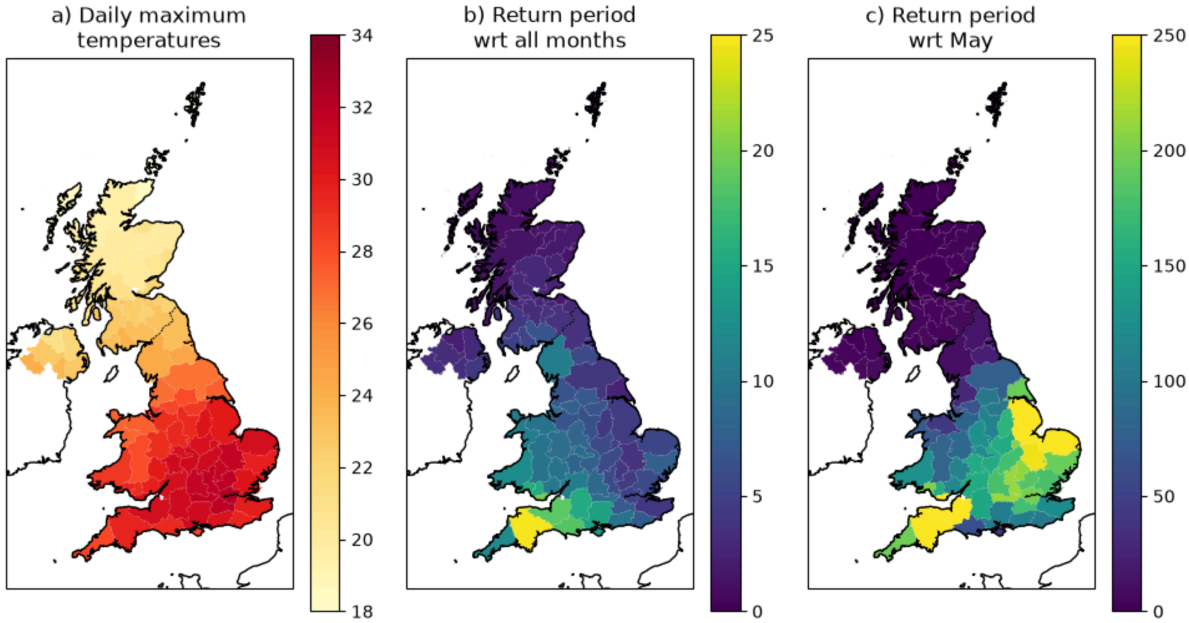

Figure 1.3: *(a) Mean of daily maximum temperatures in each county from May 24-26; (b) return period of similarly extreme temperatures at any time of the year; (c) return period of similarly extreme temperatures in May. Higher return periods indicate rarer and therefore more extreme events. Data: HadUK-Grid (provisional).*

The spatial pattern of daily maximum temperatures was similar during the June heatwave (Figure 1.4a), with consistently higher temperatures across the whole of the UK and 29 counties experiencing daily maximum temperatures of at least 32°C over the period. Such extreme temperatures are uncommon in the southwest even in the height of summer, with return periods of 15-25 years in Devon, Somerset and South Glamorgan (panel b). For similar temperatures to occur in June is extremely unusual: return periods exceeded 50 years across Wales and most of southwest and western England, reaching around 100 years in Devon, Dorset and Somerset (panel c).

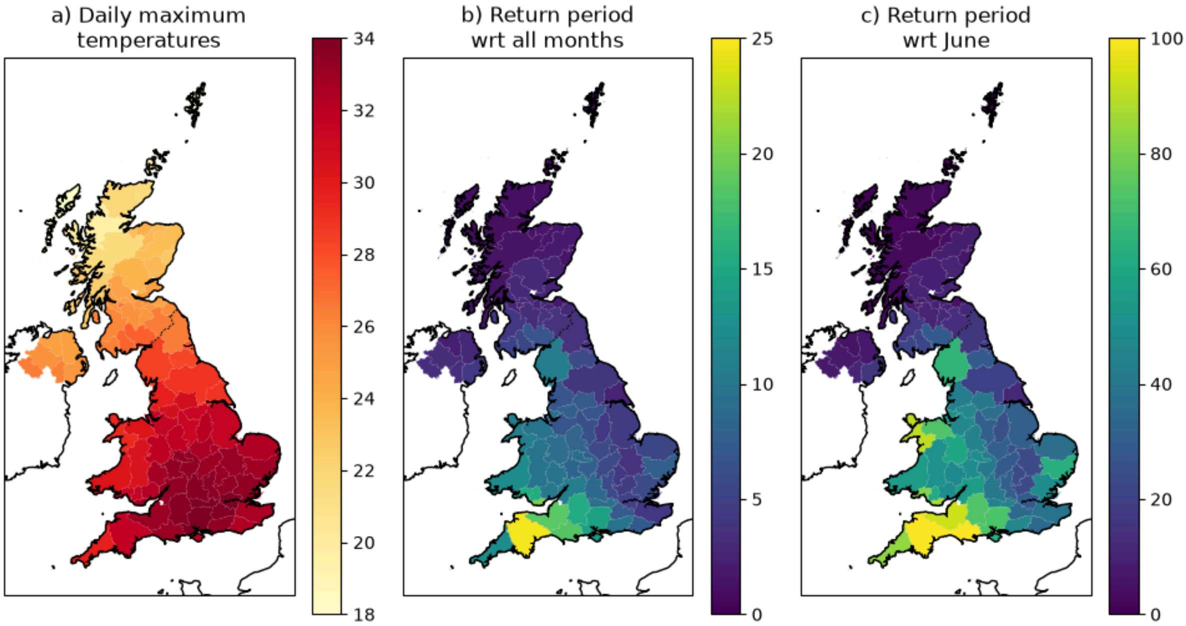

Figure 1.4: *(a) Mean of daily maximum temperatures in each county from June 24-26; (b) return period of similarly extreme temperatures at any time of the year; (c) return period of similarly extreme temperatures in June. Higher return periods indicate rarer and therefore more extreme events. Data: HadUK-Grid (provisional).*

Night-time temperatures during the June heatwave were even more extreme; in Greater London and eight counties in southern and southwestern England, 3-night average temperatures were above 20°C. Such heat would be extremely unusual at any time of year but especially in June, with return periods well in excess of 100 years across much of England and Wales, especially in the southwest (Figure 1.5).

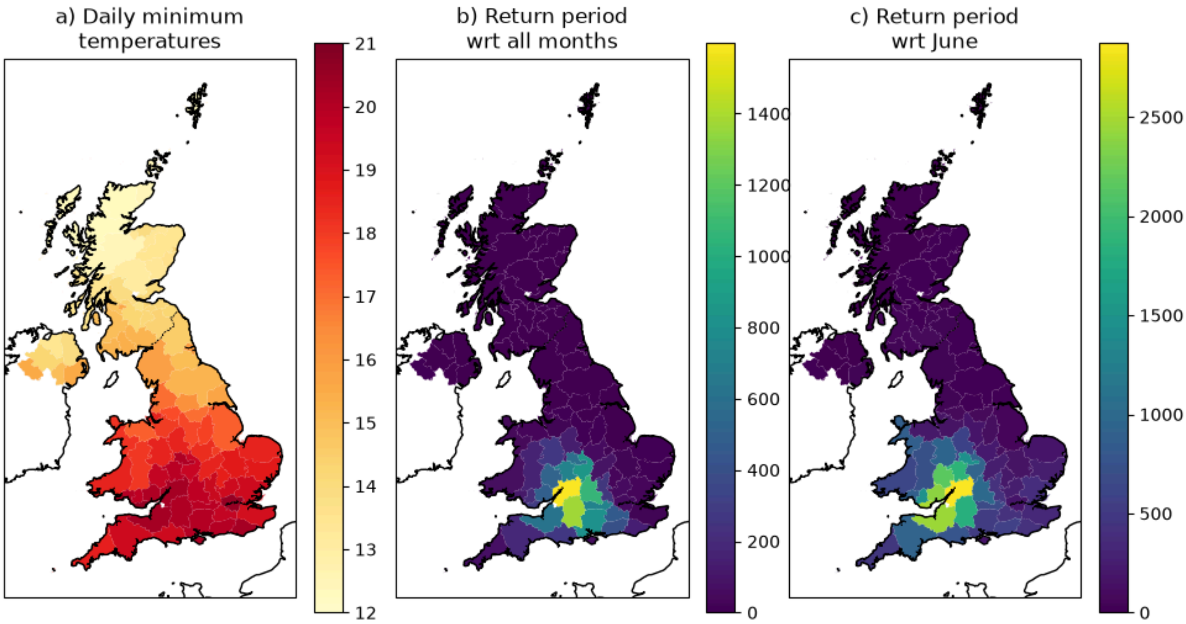

Figure 1.5: *(a) Mean of daily minimum temperatures in each county from June 24-26; (b) return*

period of similarly warm night-time temperatures at any time of the year; (c) return period of similarly warm night-time temperatures in June. Higher return periods indicate rarer and therefore more extreme events. Data: HadUK-Grid (provisional).

While much of the UK experienced unusually high temperatures during both heatwaves, this report will focus primarily on England and Wales, which experienced the highest temperatures both in absolute terms and relative to normal levels for the time of year. Part of what made this event so unusual was the size of the area experiencing extreme heat simultaneously; Figure 1.6 shows daily maximum, minimum and wet bulb globe temperatures averaged over the whole of England and Wales, contrasted with daily temperatures from 1995-2025. Both of the heatwaves stand out as far exceeding any temperatures previously experienced at that time of year, with the June heatwave also exceeding any previous event other than the record-breaking heatwave of July 2022, in terms of both daily maximum and nightly minimum temperatures. However, we note that in terms of humid heat - reflected in the daily wet bulb globe temperatures in panel c - the June event surpasses even July 2022, by around 1.4°C. Trends in extreme temperatures over the whole of England and Wales are discussed in Section 1.2, and trends in wet bulb globe temperatures are examined in Section 1.3.

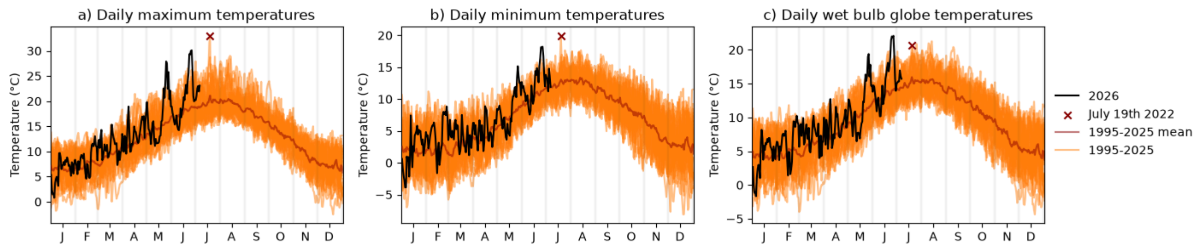

Figure 1.6: *Daily temperatures averaged over the whole of England and Wales: (a) daily maximum temperatures; (b) nightly minimum temperatures; (c) daily wet bulb globe temperatures. Black line is daily value in 2026; orange lines indicate daily values from 1995-2025; dark red is 1995-2025 mean. The value recorded on July 19th 2022 is marked with a red cross. All data: ERA5.*

1.2 Trends in extreme temperatures

1.2.1 How rare were the May and June 2026 heatwaves in the present climate?

Both 3-day maximum (Tx3x) and minimum (Tn3x) temperatures observed during May and June 2026 were extreme by the standards of the month they occurred within, but the overall estimated return periods of this event in the present day climate of 2026 depend heavily on whether we assess the likelihood of such an event in June or at some point in the year as a whole (Table 1.1). For the May event, our analysis suggests that the likelihood of an event to occur at some point during the year in the present climate is about 1 in 2 (1.4 to 3.8) years for Tx3x and almost every year for Tn3x. However, when we restrict this to assess the likelihood of occurrence in May only, the analysis suggests that such events are still exceedingly rare in the present day climate, with return periods of approximately 580 years (68 years to essentially never) for Tx3x and 60 years (15 to hundreds of thousands of years) for Tn3x. We note that because the event was so far beyond anything in the record, this should not be interpreted as a reliable quantification of the return period of similar temperatures, but as an indication of their order of magnitude.

For the June event, the difference is less stark but still highlights the rarity of the event. We estimate that the likelihood of an event to occur at some point during the year in the present climate is about 1 in 20 (8.6 to 88) years for Tx3x, and in June-only about every 101 years (27 to almost never). The 3-day minimum temperatures were so extreme that they are estimated to be almost impossible within the present climate when considering June only, though again are more likely at some point during the year, expected every 33 (9.3 to 2000) years. In part, the difference between the periods reflects the difference in sample size of extremes between using only May or June and the wider summer period, but primarily also highlights the remarkable magnitude of these events in the early summer period.

Finally, we caution that estimating the likelihood of events in the tail of the distribution or without historical precedent is challenging using the statistical methods used here (i.e. a generalised extreme value distribution with parameters estimated using maximum likelihood; described in section A1.2), as reflected in the high uncertainty ranges (Table 1.1) (Zeder et al., 2023). This challenge is further compounded by the rapid rate of warming, which is directly linked to an increased likelihood of record-breaking and record-shattering extremes (Fischer et al., 2021; Fischer et al., 2025). We therefore caution that these return periods should not be considered a concrete estimate of present day likelihood and certainly not future occurrence probability for the purposes of planning - here it is the relative return periods across different months and annual period that is primarily of interest. Such values could likely be more reliably estimated by incorporating a broader range of drivers and improved statistical techniques (Zhang et al., 2026; Risser et al., 2025). However, we note that for the purposes of attribution it is the relative likelihood of events in different climates that matters, which is not subject to the same degree of uncertainty as the assessment of fixed return periods.

Further, for the purposes of trend analysis in the following section, we further note that the choice of return period affects the estimated probability ratios but that the estimated changes in intensity are independent of this. For studying the changing likelihood of extreme heat, we use an approximate benchmark return period of 100 years (Table X1.2.2 & X1.2.3). This avoids overconfidence in the precision of our return period estimate for these specific events and facilitates comparison with other analyses.

Month	Variable	Event magnitude (°C)	Wrt annual/monthly maxima series	Return period of observed event in the 2026 climate
May	Tx3x	26.4	Annual	2.07 (1.35 to 3.77)
			May	580 (67.6 to inf)
	Tn3x	14.1	Annual	1.01 (1.00 to 1.03)
			May	59.6 (15.0 to 314000)

June	Tx3x	29.8	Annual	19.9 (8.58 to 87.8)
			June	101 (26.8 to inf)
	Tn3x	18.5	Annual	33.2 (9.25 to 1980)
			June	Inf (>18900)

Table 1.1: *Estimated return periods of May and June 3-day maximum temperatures (Tx3x) and minimum temperature (Tn3x) over England & Wales, along with the return period and associated magnitude used for trend analysis. Estimated changes in likelihood and intensity for each variable associated with global warming since 1976 (approximately 1.1°C) are shown in the right hand columns.*

1.2.2 How are summer heat extremes changing in England and Wales due to human-induced climate change?

Next, we assess the changing likelihood and intensity of the benchmark 1 in 100 year events in Tx3x and Tn3x across England and Wales associated with an increase in global temperature of 1.1°C, using four gridded observational and reanalysis datasets (see section 3.1.1). The results are clear across all datasets and for all indices; intense heat in England and Wales has become much more likely and intense as a result of this human-induced warming (Figs. 1.7 & 1.8 ; Tables 1.2 & 1.3). Fifty years ago in 1976, when the world was approximately 1.1°C cooler, such intense daily maximum temperatures would have been tens to hundreds of times less likely, with best estimates of the probability ratio ranging from around 20 to around 250 across datasets, making such an event a return period of several thousand years. Equivalently, this period of intense maximum temperatures has warmed by around 2-3°C compared to an event of equivalent likelihood in 1976, suggesting that such events are warming at double to triple the global warming rate, consistent with other findings for heatwaves in the UK and Europe.

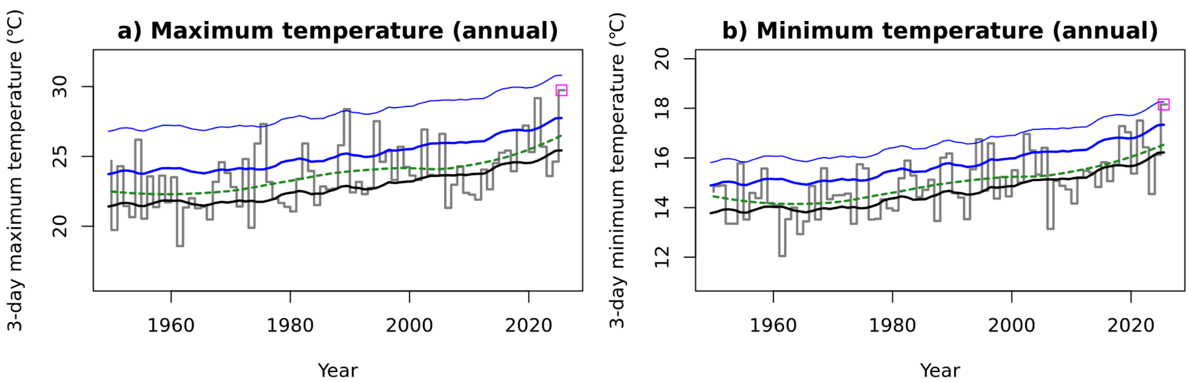

Figure 1.7: *Time series of annual Tx3x (left) and Tn3x (right)in the ERA5 reanalysis dataset for England & Wales. The June 2026 event is shown in the pink box. The loess-smoothed trend is shown*

with the green dashed line and the fitted statistical model that varies with GMST is shown with the black and blue lines, showing the fitted values (black line), and the 1-in-6 (bold blue) and 1-in-40-year (lighter blue) return period event magnitudes.

The change in likelihood for such an intense period of nighttime temperatures is even more stark. Across all datasets, we find that such an event would have been virtually impossible in the climate of 1976. Only two datasets have finite lower bounds, the lowest of which is a change in likelihood of a factor of 60. Equivalently, the extreme minimum temperatures have warmed by approximately 1-2°C compared to an event of equivalent likelihood in 1976, suggesting that such events are warming at or up to double the global warming rate. While this is a slower increase in intensity than the daytime maxima, it still results in a larger change in likelihood due to the lower variability of peak minimum temperatures (Figure 1.7). Furthermore, it remains a rapid rise by the standards of heat events globally, and hotter nights can compound the impacts of hotter days by preventing cooling and hampering rest between periods of intense daytime heat.

Tx3x (°C)	**Observed 2026 event characteristics**		**Analysed 100-year event characteristics**		**Change since 1976**	
	Magnitude	**Return period**	**Magnitude**	**Return period**	**Probability ratio**	**Change in magnitude**
ERA5	29.77	19.9 (8.60 to 88.1)	31.7 (29.9 to 34.1)	100	21.0 (3.02 to 138000)	3.08 (1.86 to 4.24)
Berkeley			33.7 (32.3 to 34.9)	100	248 (9.11 to Inf)	2.17 (1.33 to 2.98)
E-Obs			32.9 (31.0 to 34.7)	100	151 (8.11 to Inf)	2.76 (1.57 to 3.87)
HadUK-Grid			33.8 (31.6 to 36.2)	100	35.3 (4.66 to Inf)	2.89 (1.51 to 4.05)

Table 1.2: *Estimated return periods of annual 3-day maximum temperatures (Tx3x) over England & Wales, along with the return period and associated magnitude used for trend analysis. Estimated changes in likelihood and intensity associated with global warming since 1976 (approximately 1.1°C) are shown in the right hand columns.*

Tn3x (°C)	Observed 2026 event characteristics		Analysed 100-year event characteristics		Change since 1976	
	Magnitude	Return period	Magnitude	Return period	Probability ratio	Change in magnitude

ERA5	18.2	33.2 (9.25 to 1980)	18.4 (17.8 to 19.1)	100	Inf (57.9 to inf)	2.02 (1.31 to 2.60)
Berkeley			16.6 (16.1 to 17.1)	100	Inf (>1m to inf)	1.54 (1.16 to 2.00)
E-Obs			17.4 (16.9 to 18.1)	100	Inf (inf to inf)	1.05 (0.64 to 1.66)
HadUK-Grid			17.4 (17.0 to 17.9)	100	Inf (inf to inf)	1.54 (1.09 to 2.02)

Table 1.3: *Estimated return periods of annual 3-day minimum temperature (Tn3x) over England & Wales, along with the return period and associated magnitude used for trend analysis. Estimated changes in likelihood and intensity associated with global warming since 1976 (approximately 1.1°C) are shown in the right hand columns.*

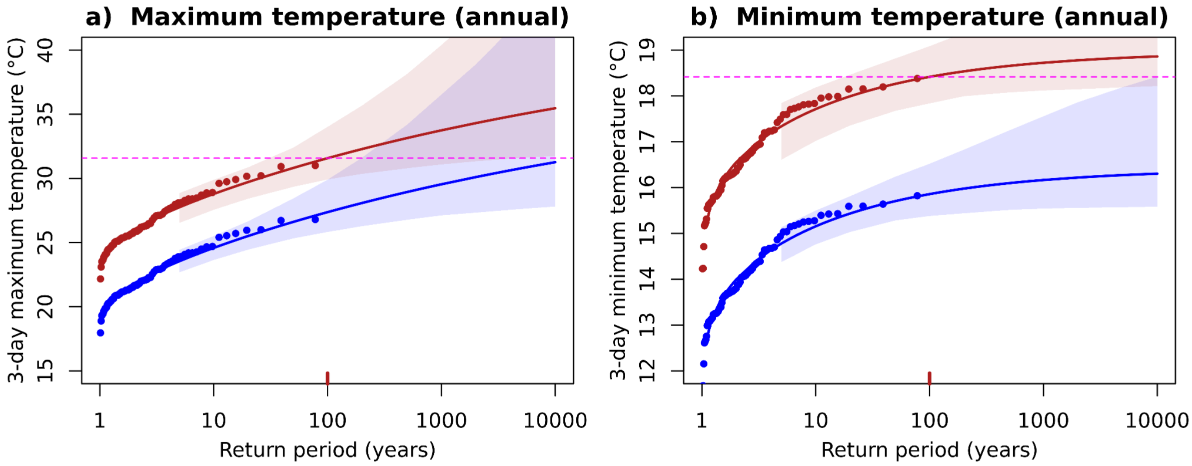

Figure 1.8: *Statistical fits to the 3-day maximum and minimum temperature time series shown in Figure 1.7. The influence of the current GMST is shown with the red vs blue probability curves, showing the present (2026) vs past 1976 warming levels. The magnitude of the 1-in-100-year event is highlighted with a horizontal purple line.*

1.2.3 HadGEM3 Large Ensemble Simulations

A recent analysis by Holliday et al., (2025) investigated the likelihood of record-breaking May temperature extremes occurring anywhere within the UK. At the time of writing the all-time maximum temperature record for May in the UK was 32.8°C, set at multiple stations in southeast England during the exceptional early-season heatwave of 1944. The authors found that anthropogenic climate change had increased the likelihood of breaking this record by around a factor of three, and inferred that an event of equivalent rarity (106 year return period) occurring in the present climate could see maximum temperatures 1.4°C higher (34.2°C) than the 1944 record. In May 2026 a temperature of 35.1°C was reached at Kew Gardens, London.

Here we extend this analysis, utilising the same underpinning methodological approach as Holliday et al., (2025), but applied to the early season heatwaves of May and June 2026. In Holliday et al., (2025) the analysis looked at the highest one day maximum temperature. In this analysis we calculate Tx3x for the England and Wales region, and fit a GEV distribution. The HadGEM3 ensemble is able to produce extremes of comparable magnitude to those observed, but both the May and June heatwaves are exceptional events for the time of year in the present day climate. For the May event the model estimates a return period of approximately 1785 years (95% CI 1075 to 3448) and for the June event a return period of 463 years (95% CI 341 to 662). Because these events are so far into the tail of the distribution as noted previously, and as noted in section 3.2 the potential for biases in some physical processes in the model, we advise caution in interpreting these values as precise estimates of the 'true' return period of the events. The remainder of this section of analysis will focus on the assessment of these in relation to their probability of occurring at any time of year (which will primarily be the summer season June to August but could include events May to September).

Within the ALL forcing simulation an event as severe as the event in May 2026 has a return period of approximately 5 years, compared to 16 years in the NAT simulation. An event of this magnitude for 3 day maximum temperatures occurring at some point in the summer season is not unusual, consistent with the findings from the observational data in Table 1.1, but it having occurred in late May is exceptional in analysis of both the historical observations and the climate model.

The June 2026 heatwave is estimated to have a return period of approximately 26 years (range 23 to 28) which compares well with an estimated 19.9 years (range 8.6 to 88.1) from ERA5 (Table 1.2). The NAT simulations estimate a return period closer to 150 years. Therefore a comparable heatwave is estimated to have become around 5.7 times more likely due to human-induced climate change. Figure 1.2.3 shows that as a 3-day heat event for daily maximum temperatures it is second only to the heatwave of July 2022, which saw temperatures exceed 40C for the first time in the UK.

The estimated change in magnitude for events of equivalent return period are 1.52°C (range 1.4 to 1.62°C) and 1.69°C (range 1.53 to 1.84°C) for the May and June events respectively (Table 1.4). These values are somewhat lower than those estimated from observations in Table 1.2, although the respective uncertainty ranges do overlap. There are a number of potential contributing reasons for this. There are differences in the statistical methodology being applied for the observational and climate model analyses in this case, meaning that the values are not directly comparable. Observed trends in extreme temperatures since the 1960s have been somewhat higher than simulated by climate models (see for example Figure 1.9), particularly a notable cluster of heat extremes in the most recent decades. The model analysis here is also based on simulated change for a recent past (2017-2024) which will also slightly underestimate the amount of climate change influencing the statistics for 2026. For this reason we expect that the model estimates of change presented here are conservative.

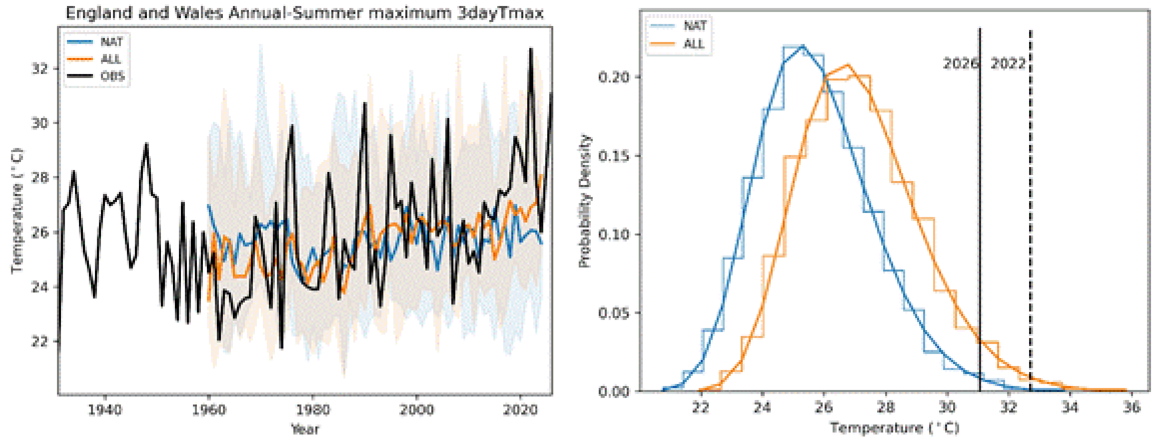

Figure 1.9: *(left) Time series of Tx3x observations 1931-2026 from HadUK-Grid (black), along with HadGEM3-A data 1960-2024 for the ALL (orange) and NAT (blue) ensembles. Solid lines show the HadGEM3-A ensemble median, and shading shows the ensemble spread for the 15-member historical ensemble. (right) show histogram and the probability density for the ALL and NAT ensembles, along with vertical lines showing the June 2026 heatwave and the July 2022 which is the highest observed summer heatwave for Tx3x at time of writing.*

		Magnitude	Return Period - ALL	Return Period - NAT	Probability ratio	Change in magnitude (°C)
May Tx3x	May	28.85	1785 (1108, 3364)	12151 (5093, 45916)	6.8 (2.4, 26.5)	0.95 (0.50, 1.42)
	Annual	**28.85**	**5.2 (4.9, 5.4)**	**16.1 (14.8, 17.7)**	**3.1 (2.8, 3.4)**	**1.52 (1.41, 1.62)**
June Tx3x	June	31.06	463 (341, 662)	7275 (3634, 23326)	15.7 (7.2, 51.7)	1.52 (1.18, 1.87)
	Annual	**31.06**	**25.6 (23.4, 28.2)**	**146.8 (119.3, 186.4)**	**5.7 (4.5, 7.3)**	**1.69 (1.53, 1.84)**

Table 1.4: *HadGEM3-A estimated return periods of 3-day maximum temperatures (Tx3x) for May and June relative to the month of occurrence or annually over England & Wales along with 95% confidence intervals in brackets. Also included are the estimated probability ratio (P_all/P_nat) and estimated change in magnitude for an event with equivalent return period to the event in P_all.*

1.3 Trends in humid heat

The Wet Bulb Globe Temperature (WBGT) measures the combined effect of environmental factors on human heat stress, and is used as a composite index, combining humidity, radiant heat (such as direct sunlight), and air movement, all of which affect the body's ability to regulate its internal temperature through sweating and heat exchange. In this study, WBGT was approximated from ERA5 maximum temperature data and dewpoint temperature data (per Zhang et al., 2024) – which means results apply best to a sheltered and shaded area, without the heating effect of direct sunlight or the cooling effect of wind. By capturing the interacting variables, WBGT provides a more physiologically relevant assessment of thermal strain, particularly during outdoor physical activity. Consequently, it is widely applied in fields such as sports science and occupational health (Grundstein et al., 2023).

The humid heat conditions in late June 2026 were an exceptional event over England and Wales. The only dataset that includes the event at the time of analysis, the ERA5 reanalysis, shows that such an event is currently expected to occur only around once in a century in June, and around once in 50 years at any point in the year (Table 1.5). However, as described in section 1.2, we caution that estimating the likelihood of events in the tail of the distribution or without historical precedent is challenging using the statistical methods used here (i.e. a generalised extreme value distribution with parameters estimated using maximum likelihood; described in section A1.2), as reflected in the high uncertainty ranges (Table 1.5) For all events, we use an approximate benchmark return period (shown explicitly in Table 1.5 for each index). This avoids overconfidence in the precision of our return period estimate and facilitates comparison with other analyses.

This is similar for the 3-day maximum temperatures in the region when we consider June only, with such events also expected only around once in a century (Table 1.5). However, when we consider the return period of a similar event at any time of the year, we find that such events would be expected around every 20 years. This reflects the difference in sample size of extremes between June and the wider summer period, but primarily the remarkable magnitude of this event in the early summer period. Meanwhile, the relative humidity conditions that co-occurred with these extreme temperatures were not themselves extreme, and would be expected most years. We use a 1.5 year return period for the relative humidity indices, meaning that such conditions should occur alongside such extreme temperatures in 2 out of 3 years.

Variable		Observed event characteristics		Analysed event characteristics		Change since 1976	
		Magnitude (°C)	Return period	Magnitude (°C)	Return period	Probability ratio	Change in magnitude (°C)
WBGT (°C)	June	24.29	108 (29.3, inf)	24.23	100	38.9 (3.00, inf)	2.38 (1.26, 3.53)
	Annual	24.29	57.2 (14.6, inf)	24.23	50	Inf (6.18, inf)	2.37 (1.46, 3.22)

Tx3x (°C)	June	29.74	91.2 (24.0, inf)	29.84	100	49.7 (2.64, inf)	3.03 (1.56, 4.55)
	Annual	29.74	20.42 (9.45, 84.6)	29.71	20	21.7 (3.36, inf)	3.30 (2.04, 4.35)
RH (%)	June	50.24	1.20 (1.05, 1.45)	54.04	1.5	0.79 (0.54, 1.02)	-4.16 (-8.15, +0.34)
	Annual	50.24	1.39 (1.09, 1.84)	51.28	1.5	0.72 (0.53, 0.99)	-6.98 (-10.9, -0.25)

Table 1.5: *Estimated return periods of WBGT and the associated 3-day maximum temperatures (Tx3x) and relative humidity (RH) values in both June-only and annually over England & Wales, along with the return period and associated magnitude used for trend analysis. Estimated changes in likelihood and intensity for each variable associated with global warming since 1976 (approximately 1.1°C) are shown in the right hand columns.*

The historical data shows a clear increasing trend in the occurrence and intensity of extreme humid heat over England and Wales (Figure 1.5). Since 1976, when the world was approximately 1.1°C cooler, humid heat events as intense as in late June 2026 would have been virtually impossible. Equivalently, humid heat events have become about 2.4°C (1.5 to 3.2°C) hotter when they occur at any time of the year; this result is remarkably consistent if we consider changes in June alone. These changes are clearly evident in the time series figures (Figure 1.10), which show a nearly-monotonically increasing trend across the record (since 1950) for both annual and June-only events, as well as the return curves (Figure 1.11). Changes since 2003 (with global warming of approximately 0.6°C) and since preindustrial conditions (with global warming of approximately 1.4°C) are shown in the appendix, but show changes consistent with those in Table 1.5.

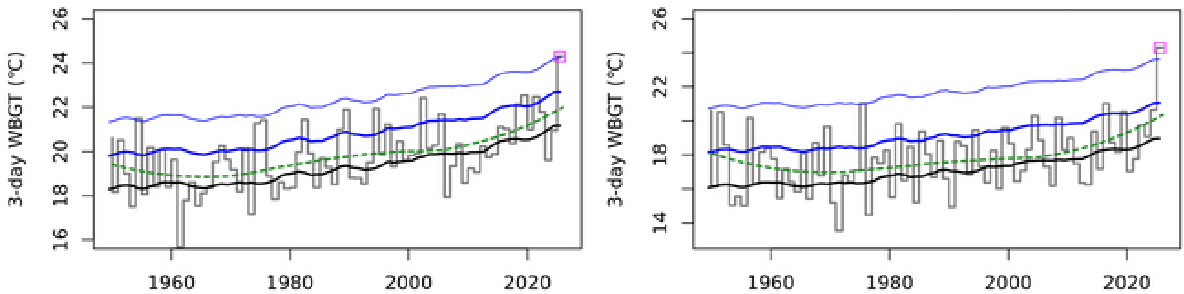

Figure 1.10: *Time series of annual (left) and June-only (right) 3-day WBGT in the ERA5 reanalysis dataset for England & Wales. The 2026 event is shown in the pink box. The loess-smoothed trend is shown with the green dashed line and the fitted statistical model that varies with GMST is shown with the black and blue lines, showing the fitted values (black line), and the 1-in-6 (bold blue) and 1-in-40-year (lighter blue) return period event magnitudes.*

This increase in humid heat is driven by the rise in daily maximum temperatures, which have warmed by approximately 3.0°C (1.6 to 4.6°C) in June in the same time period, or 3.3°C (2.0 to 4.4°C) annually. Equivalently, events of this intensity occurring at any point in the year have increased in likelihood by a factor of about 22 (3.4 to infinity), and in June by a factor of around 50 (2.6 to infinity). The time series and return curve figures for maximum temperatures and relative humidity are shown in the appendix (Figs. A1 & A2). During the most intense wet bulb globe temperature events, relative humidity appears to be falling, with such events now roughly -7.0% (-11 to -0.3%) less humid annually and -4.0% (-8.1% to +0.4%) in June even as the wet bulb temperature rises. The lower decrease in relative humidity in June compared to annually likely explains the slightly higher increase in WBGT despite a lower increase in daily maximum temperatures.

Furthermore, the marginal decrease in relative humidity is likely due to the dependence between relative humidity and air temperature, with higher temperatures increasing the moisture-holding capacity of the atmosphere. Nonetheless, the rise in wet bulb temperature clearly shows that the rise in maximum temperatures outweighs the associated fall in relative humidity, leading to more intense conditions as it pertains to a person's ability to cool via sweating.

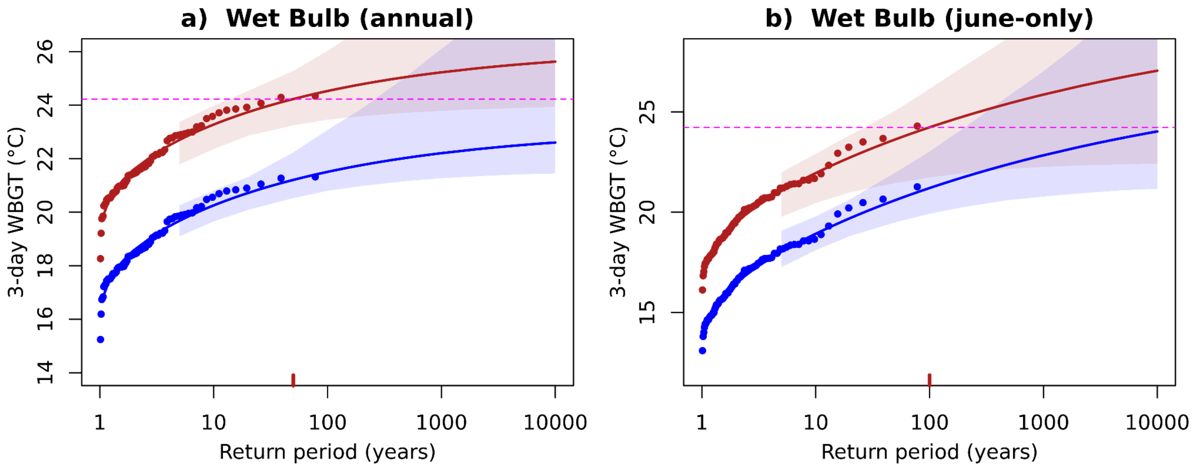

Figure 1.11: *Statistical fits to the 3-day WBGT time series shown in Figure 1.10. The influence of the current GMST is shown with the red vs blue probability curves, showing the present (2026) vs past 1976 warming levels. The magnitude of the 1-in-100-year event is highlighted with a horizontal purple line.*

1.4 Trends in monthly mean temperatures

Figure 1.12 shows the pattern of attributable warming in monthly mean temperatures across England and Wales, taking into account evidence from both historical observations and climate models; these changes are used to estimate the counterfactual temperatures used in the mortality attribution analysis in Section 2 (see Section 3.1 for details of the method used and Appendix A3 for detailed results). In both months, the synthesised warming across all counties of England and Wales is about 1.5°C on average, with individual counties ranging from 1.2 to 1.7°C. However, the spatial pattern is different; in May, there is a relatively gentle east-west gradient, while in June, warming is much more pronounced in the south-east. In both months, warming is strongest in the urban heat island of Greater London. We note that monthly mean temperatures have warmed less than the hottest temperatures; this means that the counterfactual mortality estimates given in Section 2 are higher than they would be if we used changes in peak temperatures to estimate the counterfactual temperatures, rather than changes in the monthly mean. The proportion of excess heat deaths should therefore be assumed to be a conservative estimate.

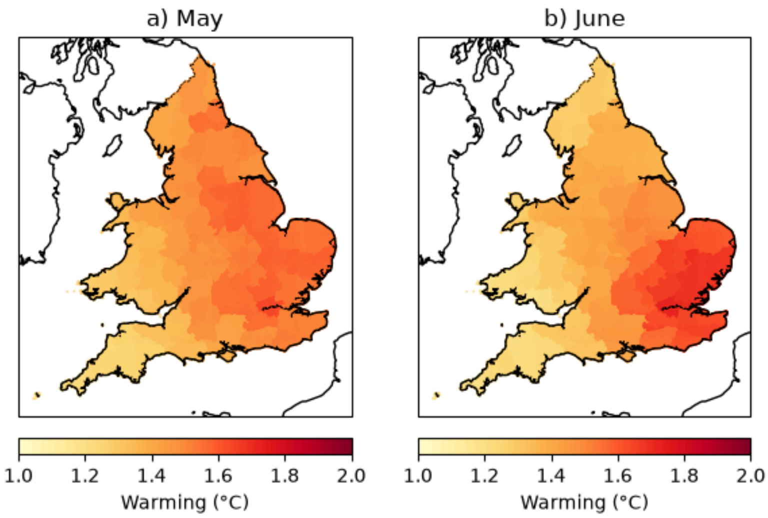

Figure 1.12: *spatial patterns of synthesised warming per county compared to a preindustrial climate with 1.4°C cooler global mean surface temperature, giving equal weight to information from observations-based products and CMIP6 climate models. a) Change in mean May temperatures; b) change in mean June temperatures.*

1.5 Summary: trends in extreme heat over the UK

The hottest temperatures reached during both the May and June heatwaves were extreme for the time of year; in the southwest the temperatures reached would be unusual at any time of year. Night-time temperatures during the June heatwave were very high, with nine counties (including Greater London) averaging night-time temperatures above 20°C for three nights (Section 1.1).

Temperatures were most extreme over England and Wales, so the remaining analysis focuses on those regions. For the region as a whole, the hottest summer temperatures are an estimated 2-3°C higher due to anthropogenic warming than they would have been in 1976, when the previous record of 35.6°C was set; multiple stations exceeded 37°C and, if verified, a new provisional record of 37.7°C at

Lingwood in Norfolk exceeded the previous record by 2.1°C. Night-time temperatures are an estimated 1-2°C warmer (Section 1.2.2).

In climate model simulations, human-caused warming due to greenhouse gases and (to a much lesser extent) land use change is estimated to have made such heatwaves 3 to 7 times more likely to occur and 1.4°C to 1.8°C more intense, although we consider this to be a conservative estimate (Section 1.2.3).

The June heatwave was particularly humid, with the highest Wet Bulb Globe Temperature (WBGT) on record when computed from ERA5 reanalysis, which extends as far back as 1950. Humid heat is more dangerous than dry heat because it impairs the body's ability to cool itself by sweating. Similarly extreme humid heat is expected to occur around once in every 50 years at any time of the year, and around once in every 100 Junes. Due to anthropogenic warming, humid heat has increased by around 2°C compared to the climate of 1976; this is driven mainly by the increase in the hottest temperatures (Section 1.3).

A full probabilistic attribution, taking into account information from both historical observations and climate models, indicates that monthly mean temperatures during May and June have warmed by around 1.5°C on average (Section 1.4). We use this estimate of the attributable warming to derive counterfactual temperatures for the heatwaves if they had occurred in a world without human-caused climate change, and so to estimate the expected number of heat-related excess deaths in the next section. However, we note that many climate models - including those used in this analysis - are known to underestimate the warming across the UK and Europe, and that this is therefore likely to be a conservative estimate of the actual warming.

2 Health impacts of changing summer temperatures

In this section, we use established exposure-response relationships (Gasparrini et al., 2022) to estimate excess mortality in all Lower-layer Super Output Areas (LSOAs) in England and Wales, given the observed temperatures (the ‘factual’ scenario) and also under the counterfactual scenario of a similarly extreme heatwave occurring in a world without human-caused warming.
The exposure-response relationships are obtained using historical mortality data (2000-2019), and an established three-step methodological framework that accounts for lagged effects and addresses data sparsity through pooled estimates and extrapolation techniques (see Section 3.3). The factual temperatures are the daily mean temperatures in each LSOA, obtained by area-weighted gridded temperature data at 1km resolution from the Met Office HadUK-Grid dataset (Hollis et al., 2019). Counterfactual temperatures are calculated by subtracting the synthesised change in temperatures in each county associated with 1.4°C of warming since the preindustrial period, as discussed in section 1.4 (see section 3.1.5 for details on the methods). By comparing these estimates, we calculate how many more people are expected to have died in each LSOA during these two heatwaves, due to the excess heat caused by anthropogenic warming. We note that a more accurate estimate of the mortality toll will be possible once the Office for National Statistics releases the finalised mortality figures for the full year in 2027.

2.1 Overall results

We estimate a total of 553 (95% empirical Confidence Intervals: 426 - 704) excess heat-related deaths during 21-29 May 2026 and 2,183 (95%eCI: 1,582 - 2,724) during 18-28 June 2026 in England and Wales (Table 2.1). Across the age groups, the largest estimated mortality impacts were observed consistently in older populations with approximately 60% of the estimated total excess deaths due to heat to be observed in populations older than 85 years of age. Out of the 553 estimated heat-related excess deaths in May, we found that 59% (95% eCI: 36% - 75%) can be attributed to human induced climate change, whereas out of the 2,183 in June 38% (95% eCI: 22% - 53%) could be attributed to human induced climate change. These proportions were found to be consistent across the different age groups. The lower proportion during the June heatwave reflects the extremeness of the temperatures, which would have resulted in very high heat-related excess mortality even without the additional contribution from human-caused warming.

Table 2.1: *Representative population (in 2024), mean and 95% uncertainty intervals of the number of excess heat-deaths under the factual scenario (observed temperatures) and counterfactual scenario (in the absence of human-caused warming); difference between factual and counterfactual scenarios; and the proportion (%) of excess heat-deaths due to anthropogenic climate change (ACC) across the different age groups during the May and June heatwaves in England and Wales.*

21-29 May					
		Expected excess heat-related deaths			
Age	**Population**	**Expected under factual scenario**	**Expected under counterfactual scenario**	**Difference**	**Proportion attributable to ACC (%)**
0-64	50,133,086	79 (40 - 124)	33 (15 - 62)	46 (17 - 77)	58 (34 - 74)
65-74	5,872,489	48 (2 - 93)	20 (3 - 44)	26 (-3 - 56)	55 (-4 - 77)
75-84	4,229,502	121 (50 - 194)	47 (20 - 92)	71 (26 - 121)	60 (38 - 76)
85+	1,571,605	304 (227 - 398)	123 (69 - 214)	178(104 - 260)	59 (36 - 76)
Total	61,806,682	553 (426 - 704)	227 (128 - 373)	327 (191 - 461)	59 (36 - 75)
18-28 June					
0-64	50,133,086	305 (106 - 476)	184 (79 - 318)	115 (23 - 205)	38 (19 - 53)
65-74	5,872,489	167 (-88 - 377)	101 (-41 - 242)	59 (-63 - 159)	37 (-48 - 78)
75-84	4,229,502	508 (162 - 807)	305 (109 - 531)	189 (55 - 343)	39 (22 - 54)
85+	1,571,605	1,225 (907 - 1,535)	756 (508 - 1088)	454 (252 - 690)	38 (22 - 52)
Total	61,806,682	2,183 (1,582 - 2,724)	1,349 (935 - 1,922)	825 (441 - 1,230)	38 (22 - 53)

2.2 Temporal variation

During the period 21-29 May 2026, the single day with the largest estimated excess heat-related mortality was 26 May, on which the estimated number of excess deaths exceeded 200, with almost half of those attributable to human-induced climate change (Figure 2.1). The estimated excess mortality due to heat in June was substantially elevated for six days, and almost 40% of the estimated heat-deaths would have been avoided in a world without human-induced climate change (Table 2.1).

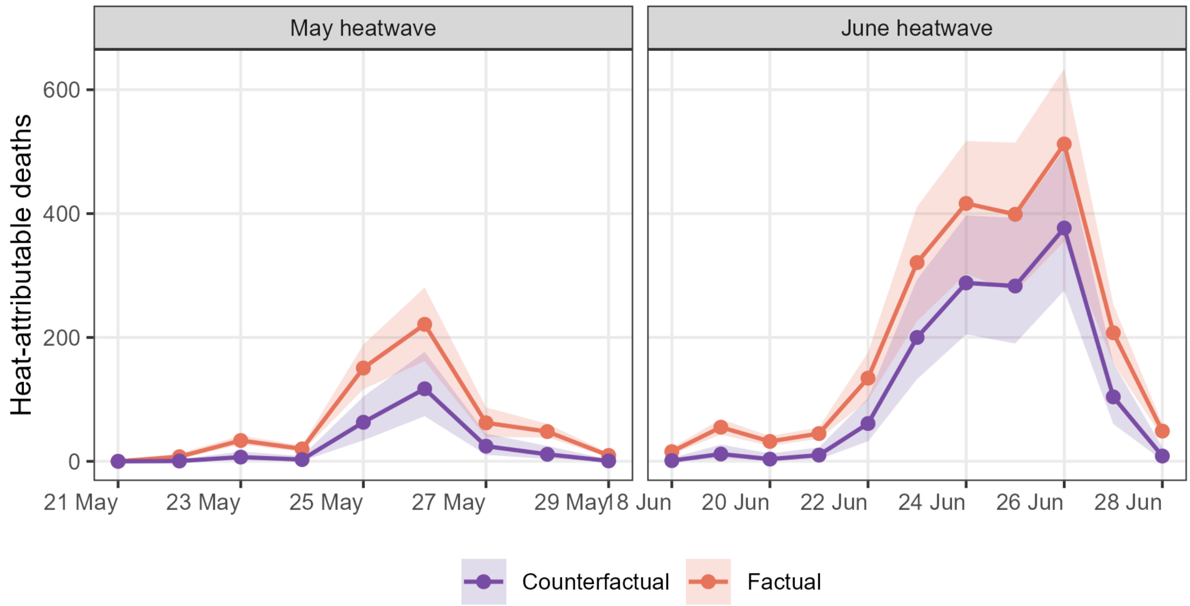

Figure 2.1: *Mean and 95% empirical confidence intervals of the estimated heat-related deaths each day under the factual and counterfactual scenarios during the May and June heatwaves in 2026.*

2.3 Spatial variation

Table 2.2 and Figure 2.2 present the regional population estimates for 2024 alongside the estimated excess heat-related deaths under both the factual and counterfactual scenarios, their absolute difference, and the proportion of heat-related deaths attributable to human-induced climate change. During the May heatwave, the highest numbers of estimated excess heat-related deaths were found in London (109; 95% eCI: 85–133) and the South East (110; 95% eCI: 81–144), with approximately 65% of these deaths attributable to human-induced climate change in both regions. During the June heatwave, excess heat-related deaths remained particularly high in London (344; 95% eCI: 272–405) and the South East (439; 95% eCI: 325–562), with the West Midlands also showing a substantial burden (301; 95% eCI: 233–361). The lowest excess heat-related mortality was observed in Wales and the North East. Notably, the proportion of heat-related deaths attributable to human-induced climate change was consistently lower across all regions during the June heatwave compared to the May heatwave. This reflects the extremeness of the June event, which would have resulted in very high heat-related excess mortality even without the additional contribution from human-caused warming.

The bottom panels of Figure 2.2 show the excess heat-mortality rate per 1,000,000 population across the regions in England and Wales and the two heatwaves. After accounting for population size, during the May heatwave the hardest hit regions per 1,000,000 population were the South West, London and the South East, whereas during the June heatwave the heat-related mortality rate per 1,000,000 population was highest in the West Midlands, South East and South West.

Table 2.2: *Representative population (in 2024), mean and 95% uncertainty intervals of the number of excess heat-deaths under the factual scenario (observed temperatures) and counterfactual scenario (in the absence of human-caused warming); difference between factual and counterfactual scenarios; and the proportion (%) of excess heat-deaths due to anthropogenic climate change (ACC); aggregated per region during the May and June heatwaves in England and Wales.*

21-29 May					
		Expected excess heat-related deaths			
Region	**Population**	**Expected under factual scenario**	**Expected under counterfactual scenario**	**Difference**	**Proportion attributable to ACC (%)**
London	9,089,736	109 (85 - 133)	40 (20 - 69)	69 (42 - 97)	64 (40 - 82)
North West	7,737,414	47 (29 - 64)	19 (10 - 32)	27 (14 - 42)	58 (38 - 74)
Yorkshire and The Humber	5,672,962	34 (22 - 46)	15 (9 - 24)	19 (10 - 29)	55 (35 - 71)
North East	2,760,678	4 (2 - 7)	1 (0 - 2)	3 (2 - 6)	87 (57 - 97)
West Midlands	6,187,204	67 (51 - 81)	31 (19 - 48)	35 (21 - 49)	53 (33 - 67)
East Midlands	5,063,164	42 (27 - 55)	20 (12 - 30)	21 (11 - 32)	52 (34 - 67)
South West	5,889,695	71 (31 - 115)	35 (14 - 66)	34 (13 - 63)	50 (27 - 69)
East of England	6,576,306	40 (29 - 52)	12 (5 - 24)	27 (17 - 40)	70 (45 - 87)
South East	9,642,942	110 (81 - 144)	38 (17 - 69)	72 (42 - 104)	65 (41 - 83)
Wales	3,186,581	30 (15 - 50)	16 (8 - 28)	14 (4 - 27)	47 (22 - 65)
18-28 June					
London	9,089,736	344 (272 - 405)	197 (130 - 276)	142 (82 - 210)	42 (24 - 58)
North West	7,737,414	216 (121 - 303)	136 (80 - 211)	78 (24 - 131)	36 (17 - 53)
Yorkshire and The Humber	5,672,962	133 (81 - 179)	73 (43 - 116)	58 (24 - 95)	45 (24 - 62)
North East	2,760,678	45 (-1 - 89)	24 (5 - 48)	21 (-5 - 50)	46 (2 - 83)
West Midlands	6,187,204	301 (223 - 361)	203 (144 - 274)	96 (45 - 146)	33 (16 - 47)
East Midlands	5,063,164	149 (92 - 197)	85 (52 - 128)	59 (29 - 94)	42 (24 - 57)
South West	5,889,695	248 (110 - 366)	170 (82 - 270)	73 (22 - 133)	30 (13 - 45)
East of England	6,576,306	218 (153 - 274)	118 (75 - 169)	98 (57 - 146)	46 (30 - 61)
South East	9,642,942	439 (325 - 562)	273 (185 - 368)	166 (93 - 246)	38 (23 - 52)
Wales	3,186,581	98 (22 - 161)	70 (22 - 121)	27 (0 - 57)	27 (-1 - 44)

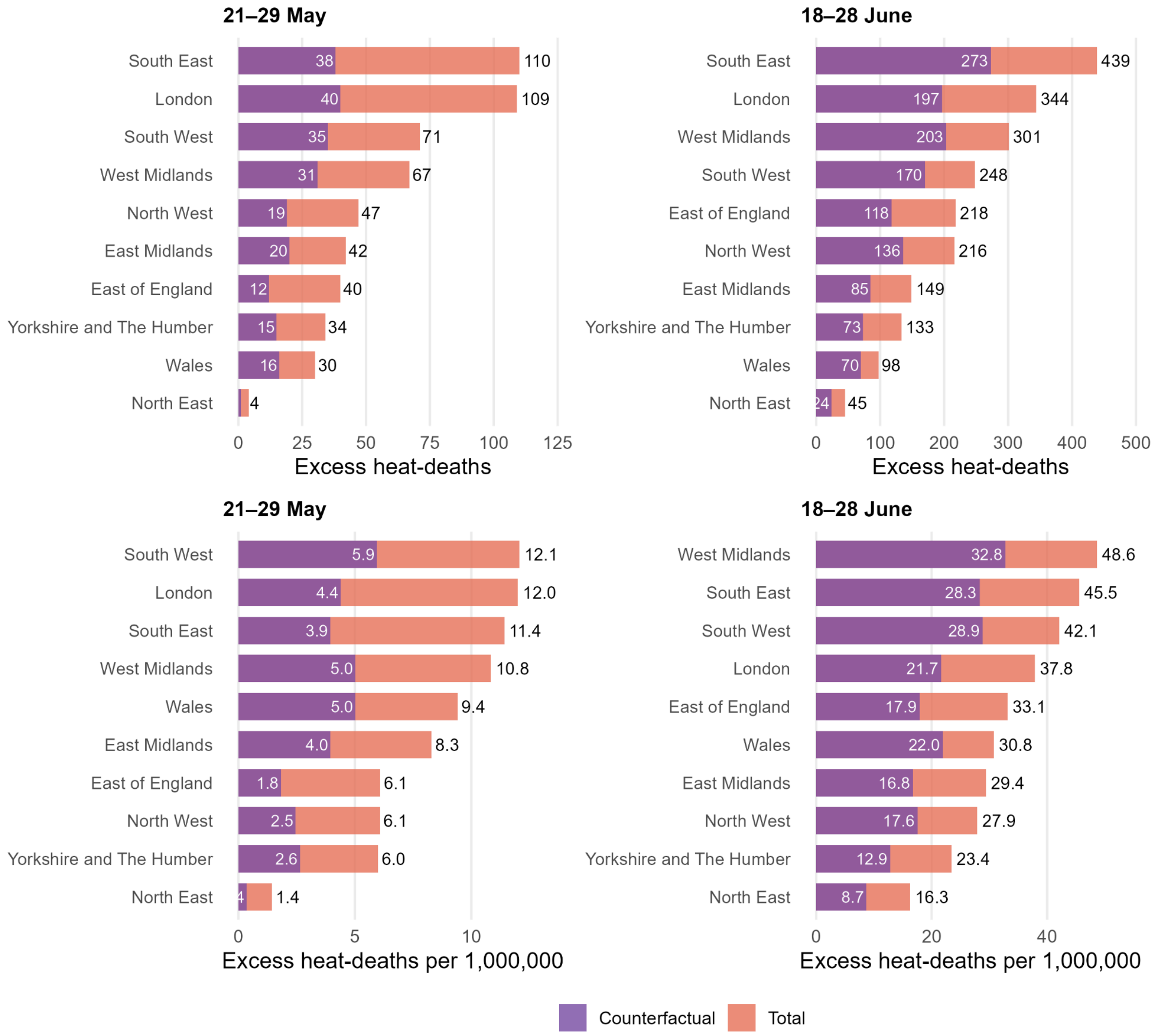

Figure 2.2: *(Top row) Mean estimated absolute factual and counterfactual heat-related excess mortality per region; (bottom row) mean estimated heat-related mortality rate (per 1 million population) during the May and June heatwaves in 2026.*

Figure 2.3 shows the spatial variation in estimated heat-related deaths per one million population under both the factual and counterfactual scenarios of non-anthropogenic warming across the different local authority districts. The observed spatial patterns are largely driven by the intensity of local temperature exposure, with the most affected regions corresponding to those experiencing the highest temperatures during each event. These spatial discrepancies can also reflect local vulnerabilities to heat-exposure, including air-pollution, green space accessibility and socioeconomic deprivation.

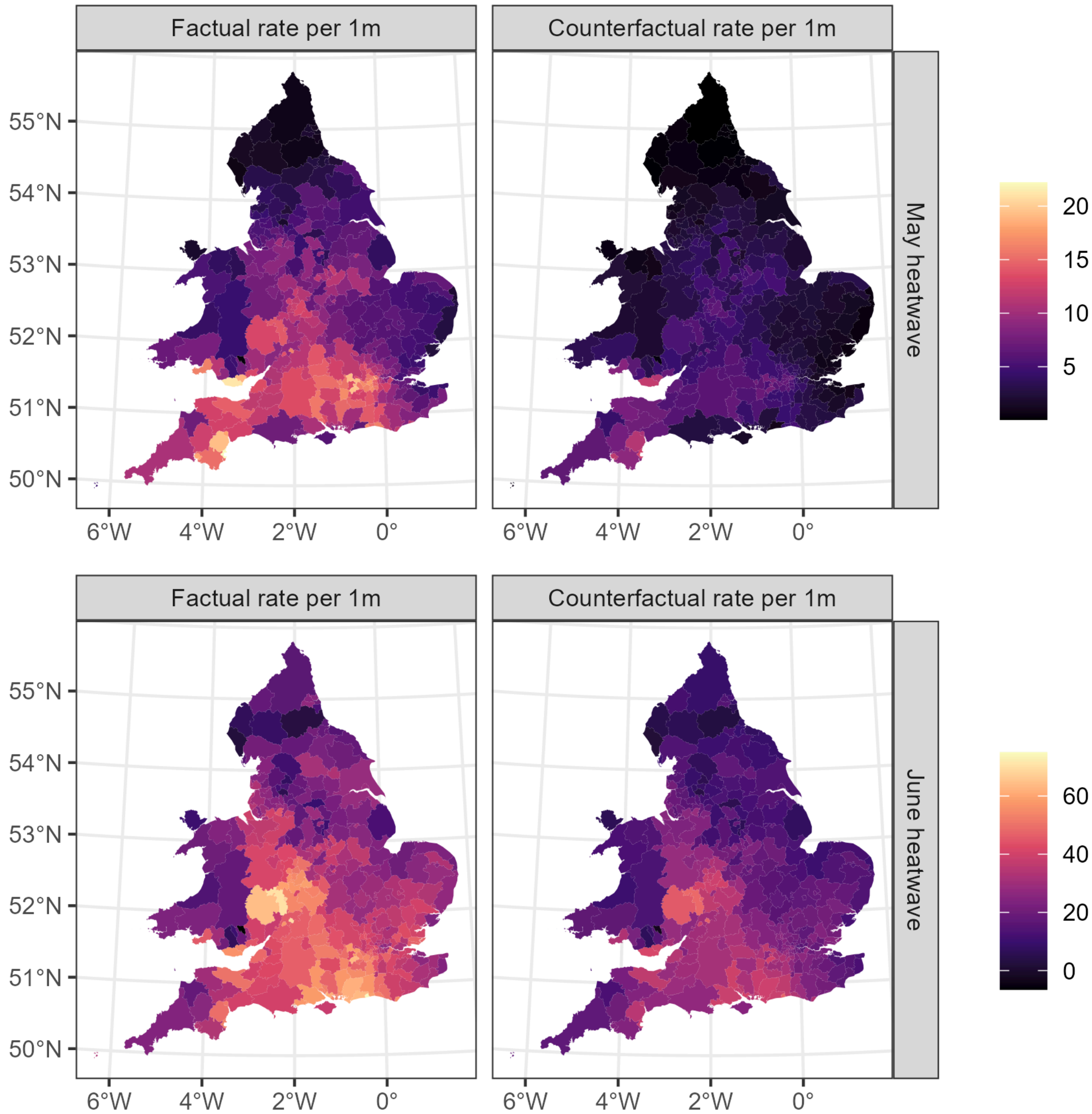

Figure 2.3: *Spatial pattern of heat-related excess deaths per million population under the factual (left) and counterfactual (right) scenarios: (top row) during the May heatwave; (bottom row) during the June heatwave.*

Emerging regional patterns in heat-related mortality

Many modelling studies identify London and the South East as the regions at greatest risk from heat-related mortality. However, as Figures 2.2 and 2.3 show, there is also a high mortality burden relative to their population size in the South West and West Midlands. Historically, London and the South East have experienced the highest temperatures and the greatest frequency of hot weather events in England, while regions in the Midlands and the North have historically experienced fewer periods of extreme heat. One explanation is that populations in regions traditionally exposed to warmer summers may have developed greater adaptive capacity through behavioural, infrastructural, and institutional responses to heat. Areas where extreme heat has historically been less common may be less prepared for prolonged periods of high temperature, potentially contributing to higher relative impacts during severe heat events. Similar emerging regional trends have been identified in recent UKHSA Heat Mortality Monitoring reports (UKHSA, 2024). Further work is required to understand the drivers of these regional differences and to determine whether the patterns observed in recent monitoring reports represent a persistent shift in heat-related health risk in England.

2.4 Comparison with previous approaches

To illustrate how consistent the results of the method used here are with estimates derived from other approaches, Table A2 presents estimates of heat-related deaths from UKHSA reports over the past four years, alongside findings from a rapid assessment of the early June 2025 heatwave, and peer-reviewed estimates for the July 2022 and August 2003 heatwaves.

To support comparison across studies, it is important to distinguish between the main methodological challenges and the different approaches used in the literature. A central challenge in estimating heat-related mortality is that heat is rarely recorded as the primary cause of death on death certificates. With the exception of heatstroke, which is a specific medical diagnosis with an ICD (International Classification of Diseases) code, heat more often acts as a trigger for other fatal events, particularly among people with chronic conditions. In such cases, the chronic disease is typically recorded as the main cause of death rather than the heat exposure that precipitated it. As a result, official counts of heat-specific deaths substantially underestimate the true mortality burden of heat.

Several modelling approaches have therefore been developed to estimate heat-related mortality more realistically. The first, which we refer to as *excess with respect to a reference period*, was widely used during the COVID-19 pandemic. This approach uses historical mortality data from the same time of year to estimate the number of deaths that would be expected had the event not occurred, without making explicit assumptions about the relationship between the event and health. The event of interest may be an extreme heatwave or an unusually hot summer, but in all cases the key idea is to identify mortality in excess of what would have been expected based on past trends. Different studies have defined the reference period differently. Konstantinoudis et al. (2025) used the period 2011-2021 to predict the mortality impacts of the extreme summer of 2022 in Switzerland, whereas since 2020 the UKHSA uses 14 days before and after the event as the reference period.

The approach used here, referred to as *parametric temperature-mortality curves*, combines historical health and temperature data within an epidemiological modelling framework to derive the association between temperature and mortality. This produces a parametric temperature-mortality relationship, which can then be applied to newly observed temperatures - including counterfactual temperatures, as we have done here - to estimate the expected number of deaths attributable to heat.

Both methods have important strengths and limitations, and they are best viewed as complementary rather than competing approaches. Estimating the excess with respect to a reference period is particularly well suited to describing extreme events and has the advantage of not requiring assumptions about the functional form of the hazard-mortality relationship. For heatwaves, this approach naturally accounts for potential adaptation to heat over time, along with seasonal variation in risk, such as during an early-season heatwave or when humidity exacerbates heat-related impacts. However, the lack of a parametric relationship makes it challenging to quantify expected mortality impacts in counterfactual temperature scenarios. This approach also depends on observed mortality data, which are not immediately available, making it less useful for early warnings or near-real-time assessment. In addition, it implicitly assumes that all excess deaths during the period of the extreme event are attributable to the event and not to other coinciding factors. Because the method relies on a recent reference period, some of the effect of rising temperatures may also already be embedded in the estimates.

Parametric temperature-mortality models can provide geographically detailed estimates of the effect of heat on mortality. Compared with historical trend extrapolation, this approach depends more heavily on assumptions about the functional form of the temperature-health relationship and may not fully capture seasonal or long-term variation in vulnerability (although it can be extended to do so). Its main advantage is that it aims to estimate deaths directly attributable to heat and can be used to assess impacts beyond only the most extreme events. This method is also often combined with weather forecasts and baseline mortality estimates to produce early estimates of the likely mortality burden of impending heatwaves for planning purposes. The accuracy of these forecasts, however, depends on both the quality of the weather predictions and the assumption that underlying mortality rates remain stable as they were during the years used to calibrate the model. Changes in population vulnerability as well as effective adaptation measures may cause a divergence from these historical rates, representing a source of uncertainty in the predicted expected excess deaths.
Previous studies in England have compared these two approaches and found broadly similar results (Mistry et al., 2024, Lo et al., 2022). However, the extent of agreement between methods is likely to depend on the characteristics of the event being studied. In the absence of a definitive “true” measure of heat-related mortality, both approaches should be used in a complementary way, and their results interpreted in light of their underlying assumptions and the nature of the event under investigation. For example, we note that a more accurate estimate of the mortality toll will be possible once the Office for National Statistics releases the finalised mortality figures, although due to the level of validation required, the final numbers will not be available until 2027.

2.5 Comparison of results with previous events

In this report, we applied the parametric temperature-mortality curve approach, using observed temperature data and assuming constant mortality rates, as finalised mortality data were not yet available at the time of the study. We estimate 553 heat-related deaths during the May heatwave (95% eCI: 426–704) and 2,183 heat-related deaths during the June heatwave (95% eCI: 1,582–2,724), Figure 2.4a. On Panel (b) we show that these approaches in general yield similar estimates for previous events.

The estimated mortality burden associated with the May heatwave is comparable to that of the most extreme heat event in July 2024 and the early heatwave in June 2025, Figure XX. The June 2026 event, however, ranks among the top two deadliest heat events and is comparable in scale to the extreme August heatwave in 2003, exceeding the estimated excess mortality from even the record-breaking heatwave of July 2022. This reflects the fact that, while the temperatures during June 2026 peaked at a slightly lower temperature than the July 2022 record, the hottest temperatures persisted for several days, with daily mean temperatures over England and Wales exceeding 22°C for four consecutive days; in July, daily mean temperatures exceeded 22°C for only two consecutive days.

We estimate that 60% of deaths during the May event were attributable to human-induced climate change, a proportion similar to that reported for Mediterranean countries by Barnes et al. (2025). In June, this proportion was around 40%; this reflects the fact that the temperatures would have been extreme - and excess mortality correspondingly high - even without the additional contribution from climate change. This estimate is also lower than that reported in our rapid assessment of 854 cities last year (Barnes et al., 2025).
As climate models are known to underestimate warming across Europe, the attributable warming is assumed to be a conservative estimate, so this analysis may therefore represent lower bounds on the true contribution of human-induced climate change.

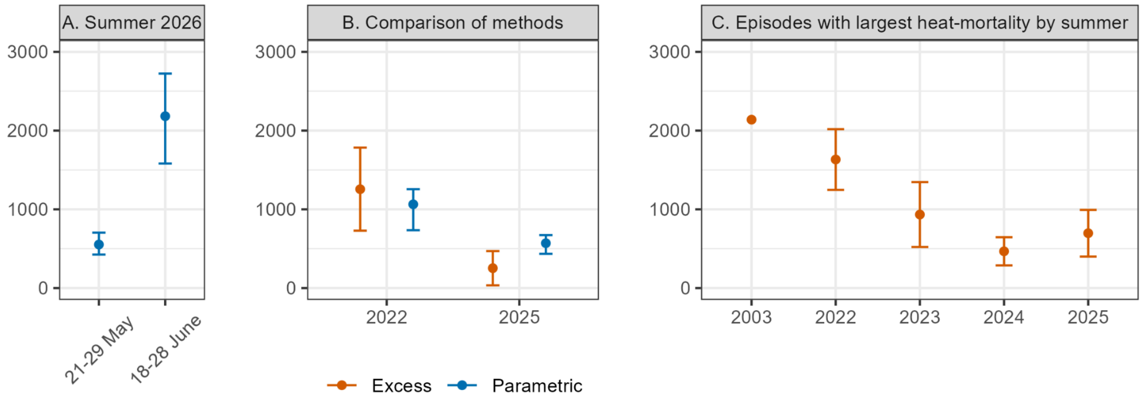

Figure 2.4: *Comparison of heat-related deaths with previously reported estimates, using two different methods: blue bars are derived from parametric exposure-response relationships (the method used in this study) and red bars estimate the excess with respect to a historical baseline (UKHSA approach). (a) estimates of the May and June 2026 heatwaves; (b) comparison of estimates for heat events that have previously been evaluated using both methods: July 10-25 2022; June 19-22 2025; (c) 4-13 August 2003 heatwave, together with the heat episodes associated with the highest mortality in UKHSA reports since 2022. For more details about the events and the related studies see Table A2.*

3 Data & methods

3.1 Data and methods used in probabilistic attribution

In Section 1 of this report, we study the influence of anthropogenic climate change on average summer temperatures by comparing the likelihood and intensity of similar weather conditions at present with those in a 1.4°C cooler climate without human-caused warming (based on Forster et al., 2026). The data and methods used in this section are described in detail below.

3.1.1 Observational datasets

The 'observed' temperatures for each city are extracted from the gridded datasets by selecting the closest grid cell to the coordinates of the city.
The observational datasets used are as follows:

- **HadUK-Grid** - a long-running collection of gridded climate variables informed by land surface observations across the UK. Meteorological observations are interpolated onto a uniform grid at 1km x 1km resolution to provide complete and consistent coverage across the UK land area (Hollis et al., 2019). Data prior to 2025 are taken from version 1.3.1; data for 2025-2026 were provisional at the time of writing. The dataset provides daily maximum and minimum temperatures, along with monthly means; to obtain daily mean temperatures, we take the mean of the daily maximum and minimum temperatures in each grid cell.

- **ERA5** - The European Centre for Medium-Range Weather Forecasts's 5th generation reanalysis product, ERA5, is a gridded dataset that combines historical observations into global estimates using advanced modelling and data assimilation systems (Hersbach et al., 2020). We use daily mean temperature data from the ERA5 product at a resolution of 0.25° × 0.25° from January 1950 until the end of May 2026, supplemented with ECMWF analysis data from June 1st-30th.

- **E-OBS (v33.0e + pre1950)** - This is a gridded land-only dataset covering Europe, derived from the interpolation of station-derived meteorological observations (Cornes et al., 2018). We use daily mean temperature data from this product at a resolution of 0.25° × 0.25°, from January 1920 to May 2026.

As a measure of anthropogenic climate change we use the global mean surface temperature (GMST), where GMST is taken from the National Aeronautics and Space Administration (NASA) Goddard Institute for Space Science (GISS) surface temperature analysis (GISTEMP, Hansen et al., 2010 and Lenssen et al. 2019). To reduce variability in the GMST due to the El Nino-Southern Oscillation (ENSO), we use a four-year rolling average of the GMST, centred on the third year.

3.1.2 Climate models

In the attribution of monthly mean temperatures used to generate counterfactual temperatures for the mortality analysis (discussed in Section 1.4), we use a multi-model ensemble of coupled global circulation models from the CMIP6 experiments (Eyring et al., 2016). For all simulations, the period 1850 to 2014 is based on historical simulations, while the SSP5-8.5 scenario is used to project from 2015 to 2030. All years from 1850 to 2030 were used to estimate the historic warming trend. 38 models were used in the analysis, each providing one realisation to the multi-model ensemble. In previous studies all models have been found to perform reasonably well in terms of capturing the seasonal cycle of temperatures over the UK, and as well as possible given the low resolution of the models at capturing the spatial pattern, so models were selected for inclusion in the analysis on the basis of how well they capture the shape of the distribution of monthly mean temperatures across all counties. Details of the models included in the study can be found in Table A2 in the Appendix.

3.1.3 Statistical modelling of trends

Methods for observational and model analysis in Section 1.4, and for synthesis of the results, are used according to the World Weather Attribution Protocol, described in Philip et al., (2020), with supporting details found in van Oldenborgh et al., (2021), Ciavarella et al., (2021), Otto et al., (2024) and here. The key steps are: trend estimation from observations; attribution using climate models; and synthesis of the attributable change in temperature. The observations-only analysis in sections 1.1, 1.2 and 1.3 use only the first stage of the protocol and do not carry out a full attribution using climate models. Section 1.4 uses the full protocol to estimate the attributable change in monthly mean temperatures for May and June, which is then used to estimate counterfactual temperatures for the mortality modelling in Section 2.

Extreme temperatures (Tx3x, Tn3x and WGBTx3x) are modelled using a Generalised Extreme Value (GEV) distribution, while monthly mean temperatures are modelled using a Gaussian distribution. In all cases, temperatures are assumed to increase linearly with global mean surface temperature (GMST), while the variance remains stationary. The parameters of each distribution are obtained using maximum likelihood estimation, with 95% confidence intervals for all quantities of interest obtained by bootstrapping, using a sample size of 1000.

3.1.4 Synthesis of trends from observations and climate models

The probabilistic attribution in Section 1.4 combines information from both observational data products and climate models. The aim was to obtain an estimate of the attributable warming per LSOA; however, for the sake of computational efficiency, the initial model fitting was carried out at county level for observational datasets, and for the CMIP6 models (many of which are so low-resolution as to represent the UK with only a handful of grid cells) at grid cell level. The fitted trend parameters for the models were then averaged over each county before being synthesised with the results from the observational analysis as described in Otto et al. (2024). Typically under the WWA protocol, the overall results from the two sets of information - models and observations - are weighted according to the precision of their respective estimates, but almost all climate models have been found to underestimate rates of warming across Europe and the UK (eg. Vautard et al., 2023; Schumacher et al., 2024), so in this analysis we give equal weight to the results from the observation-based and model-based results, rather than weighting the somewhat overconfident models more heavily. We note that this still results in a lower estimate of attributable warming than the historic warming in observations (see Appendix A3), and should therefore be interpreted as a conservative estimate.

3.1.5 Calculating counterfactuals

Factual daily mean temperatures for May and June were taken from HadUK-Grid provisional data at 1km resolution. The gridded data was averaged per LSOA using an area-weighted mean. As noted in Section 3.1.4 above, the rate of warming per calendar month was estimated independently per county.

To obtain a proper quantification of the uncertainty in the mortality estimates arising from uncertainty in the attributable warming, it is necessary to obtain a spatially coherent sample from the warming rates. To achieve this, we estimate the correlation matrix, **C**, between the rates of warming in all counties from the bootstrap samples used to estimate the model parameters from the HadUK-Grid ('factual') dataset. We then sample 1000 realisations from a multivariate normal distribution with standard normal marginals and correlation matrix **C**. Finally, the marginal distributions are transformed to have the same mean and variance as the synthesised trends. This results in a spatially coherent sample of the synthesised warming in each county, with the same correlation structure as the observed rate of warming.

Each LSOA was then assigned to a county and a sample of 1000 counterfactual temperatures across England and Wales was obtained by subtracting the sampled rate of warming per LSOA per calendar month from the factual temperatures.

3.2 Data and methods used in HadGEM3 Large Ensemble Simulations

For the attribution analysis with HadGEM3-A observational data from the HadUK-Grid (Hollis et al. 2019) is used to define the event. The daily temperature series from HadUK-Grid has been extended since the publication of Holliday et al. (2025) to now span the period 1931-present. In this analysis statistics for the 3 day average of England and Wales averaged daily Maximum Temperature (Tx3x) are used to define the event.

For the climate model analysis we have used the Met Office HadGEM3 large-ensemble system for the probabilistic attribution of extreme events. The model configuration is described by Ciavarella et al. (2018) and evaluated by Vautard et al. (2018). The model has a nominal resolution of 60km (referred to as N216) and uses observed Sea Surface Temperature (SST) and Sea Ice Concentration (SIC) as a lower boundary.

The HadGEM3-A model is run in two configurations. An ALL experiment uses anthropogenic forcings from greenhouse gas concentrations, aerosols, and land use following the fifth phase of the coupled model intercomparison project (CMIP5) using historical data to 2005 and Representative Concentration Pathways (RCP) 4.5 projections (Christidis et al., 2018) from 2005 to present. A NAT ensemble uses pre-industrial greenhouse gas concentrations and aerosols but includes estimates of natural forcings from solar and volcanic activity. NAT uses naturalised SST and sea- ice boundary as described by Christidis et al. (2013) to remove estimated anthropogenic warming but retain patterns of variability (e.g. ENSO variability). 15 member historical simulations from 1960-2013 are used for assessing trends, and model evaluation. Larger 525 member ensembles from 2017-2024 are used for the probabilistic evaluation of extremes, including model evaluation and bias adjustment as described in Holliday et al. (2025). This provides 4200 (8x525) simulated years and 126,000 (8x525x30) simulated days for a given month. Differences between the ALL and NAT ensembles represent simulated anthropogenic influences on the event's probability and intensity. The use of a sample of 8 years expands the sample size, which is valuable for capturing rare but plausible extreme events, but it does mean that the statistics are derived for a near-recent past and therefore may slightly underestimate the influence of anthropogenic forcings and climate change in 2026.

The HadGEM3-A system has been widely used in attribution studies, but it should be acknowledged that it is a single-model approach. While the model has been shown to reproduce well the main observed weather patterns responsible for European temperature extremes, as with all models there are biases found in many physical processes. For European heatwaves excessive drying of soils in the model may cause an overestimation of intense summer heatwaves (Vautard et al. 2018). For the UK a persistent underestimation of daily Tmax is removed through a mean bias adjustment of ~2.5℃ (Holliday et al. 2025)

The event likelihoods are estimated through a Generalised Extreme Value (GEV) distribution which is fit separately to each of the ALL and NAT simulations. The location and scale parameters can differ between the ensembles, allowing the width of the distribution to also change between the experiments. The uncertainty in the fit is estimated using bootstrapping (Pirret et al. 2023) the original values are sampled at random with replacement until there is a set of values the same size as the original, and the resulting set of values undergoes fitting the GEV and recalculating the probability, 1000 times. This means that the quoted uncertainties reflect the uncertainty in the statistical fit to the model data sample, but do not encompass wider uncertainties relating to model error.

The intensity change is estimated from the HadGEM3 simulations by determining the magnitude of an event in the ALL and NAT simulations with return period equivalent to the event in the ALL simulations. This has the advantage of using large-samples to capture plausible extremes in both the ALL and NAT simulations, and accounting for change in both the location and scale of the GEV fit. However it is limited by being representative of a recent past period (2017-2024) rather than present day and therefore will slightly underestimate the current or near future level of climate change.

3.3 Data & methods used in mortality attribution

To estimate the number of heat-related deaths attributable to human-induced climate change, we used a framework that combines temperature-mortality exposure-response functions with temperature time series under both factual and counterfactual climate scenarios. The approach involves three main stages. First, we retrieved the exposure-response functions by age and small area from the literature (Gasparrini et al., 2022). These functions describe how mortality risk changes with temperature and provide the basis for estimating heat-related mortality under different climate conditions. Second, we estimated heat-related mortality under factual and counterfactual temperatures. For each scenario, the exposure-response functions were applied to daily temperature series to calculate excess mortality associated with heat. This allowed us to estimate the mortality burden that occurred under observed conditions and compare it with the burden expected in the absence of human-induced climate change. Third, we attributed heat-related deaths to climate change by comparing the estimated excess mortality under the two scenarios. The absolute difference gives the number of deaths attributable to human-induced climate change, while the relative difference can be used to express the fraction of heat-related mortality attributable to anthropogenic warming.

Step 1: Exposure-response functions

The exposure-response functions were based on daily mortality records from the Office for National Statistics (ONS) across 34753 lower super output areas (LSOAs) for the period 2000-2019. Daily mean temperature data were taken from the HadUK-Grid database for the same period. Associations between temperature and mortality were estimated separately by small area and by age group (0–64 years, 65-74 years, 75-84 years, and 85 years or older), allowing for differences in vulnerability across locations and demographic groups.

Step 2: Estimation of heat-related mortality

For both factual and counterfactual temperature series, relative risks were derived and converted into attributable fractions of mortality following the methods described by Vicedo-Cabrera et al. (2023) and Beck et al. (2024), including the lagged effects of heat exposure. Daily mortality during the heatwave period was estimated using the observed mortality in 2023.

Step 3: Attribution to human-induced climate change

The number of heat-related deaths attributable to anthropogenic climate change was calculated as the difference between excess deaths estimated under the factual and counterfactual scenarios. We also estimated the proportion of total heat-related mortality in the factual scenario that could be attributed to human-induced climate change, following Beck et al. (2024).

3.3 Limitations of the method

The rapid nature of this analysis precluded access to observed death counts for England and Wales. We therefore used age-specific mortality data from 2023 at the LSOA level and assumed a constant mortality rate throughout the year. Because mortality typically rises during heatwaves, the true death rate during these periods is likely to be higher than the constant rate assumed here, which may lead to an underestimation of the absolute mortality burden attributable to heat. This limitation does not affect relative estimates, which are independent of the assumed baseline mortality rate.

Our analysis also does not account for potential adaptation to heat over time. The exposure-response functions used in this study were estimated using mortality data from 2000-2019 and may therefore not reflect any subsequent attenuation in the temperature-mortality relationship reported in the literature (Vicedo-Cabrera et al., 2018). However, there is limited evidence of adaptation to heat in the UK between 1985 and 2012 (Vicedo-Cabrera et al., 2018). If substantial adaptation to heat has occurred since 2012, then the model would likely overestimate the excess mortality.

A further limitation is that the study does not account for seasonality in heat effects. Previous research has suggested that heatwaves occurring early in the warm season may have greater health impacts than heatwaves of similar intensity later in the summer, when populations may be better acclimatised (Kalkstein & Smoyer, 1993; Anderson & Bell, 2010). Here, we assume that the temperature-mortality relationship is constant across months, and therefore do not capture potential within-season differences in vulnerability. Not accounting for this seasonality could result in an underestimation of the estimated mortality in May.

Finally, climate models are known to underestimate the rate of warming across much of Europe (e.g. Vautard et al., 2023; Schumacher et al., 2024). This implies that the estimated temperature changes attributable to anthropogenic warming may be conservative, and that the resulting estimates of climate-change-attributable mortality may also represent lower bounds.

Data availability

All data used in the attribution analysis are available on request.

Acknowledgements

This work used JASMIN, the UK's collaborative data analysis environment (https://www.jasmin.ac.uk), and Imperial College Research Computing Service, DOI: 10.14469/hpc/2232.

High-resolution provisional observations of both heatwaves were provided by the Met Office. Climate model data and other historical observations were obtained from the Deutsches Klimarechenzentrum (DKRZ), using resources granted by its Scientific Steering Committee (WLA) under project ID bk1088, and the KNMI Climate explorer web tool (https://climexp.knmi.nl/start.cgi).

References

All references are given as hyperlinks in the text.

DOI: https://doi.org/10.25560/131199

Appendices

A1 Trends in components of humid heat

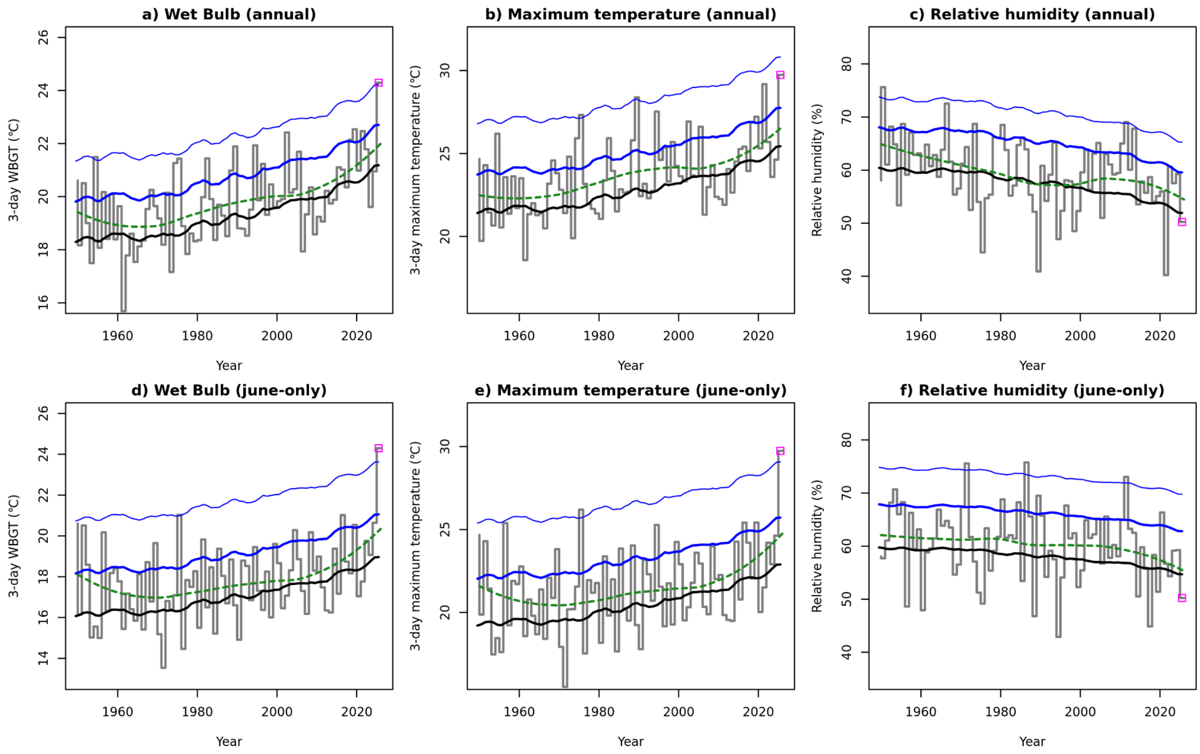

Figure A1: *Time series of annual (top) and June-only (bottom) components of extreme humid heat in the ERA5 reanalysis dataset for England & Wales: Wet Bulb Globe Temperature (left; panels (a) and (d)); 3-day averaged daily maximum temperature on the days of maximum WBGT (middle; panels (b) and (e)); 3-day averaged relative humidity on the days of maximum WBGT (middle; panels (c) and (f)). The 2026 event is shown in the pink box. The loess-smoothed trend is shown with the green dashed line and the fitted statistical model that varies with GMST is shown with the black and blue lines, showing the event (black line), and the 1-in-6 (bold blue) and 1-in-40-year (lighter blue) return period event magnitudes.*

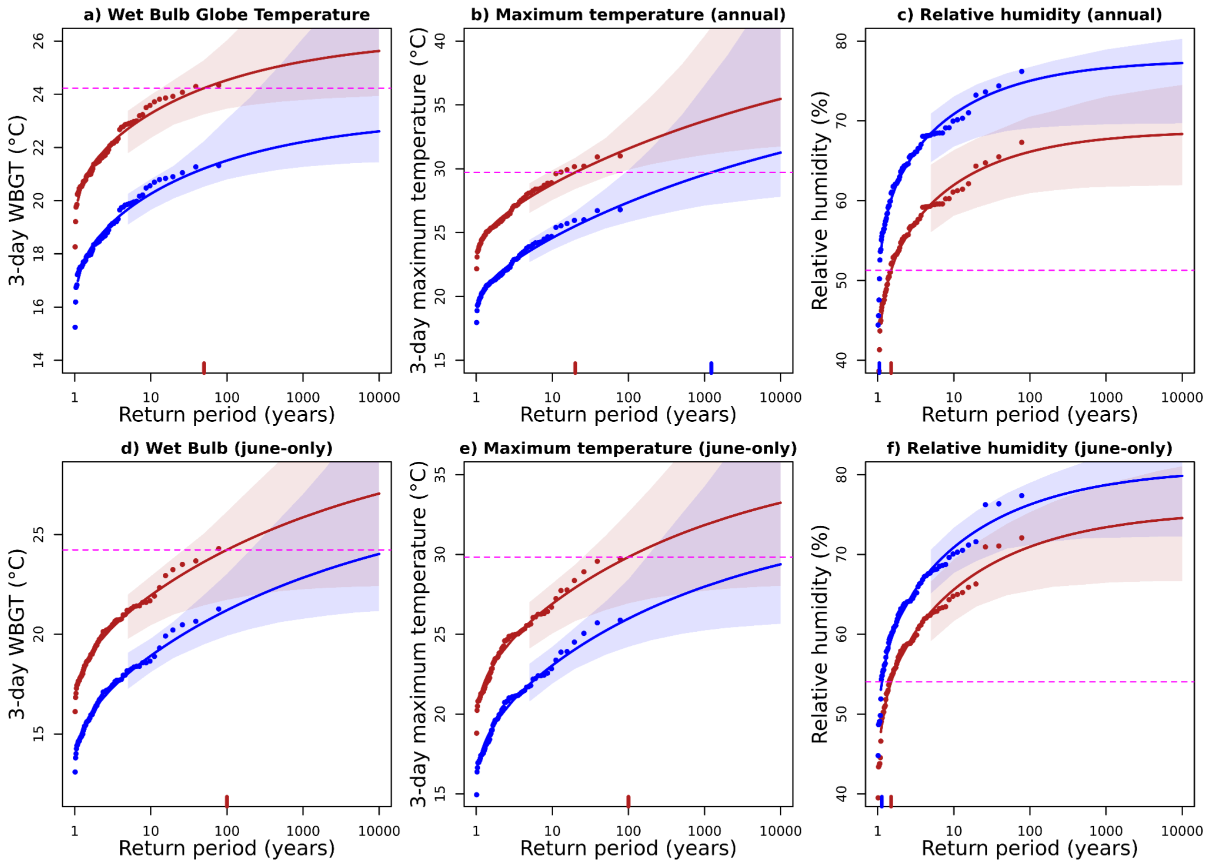

Figure A2: *Statistical fits to the three variables described in Figure A1: a & d) WBGT; b & e) 3-day maximum temperature; c & f) Relative humidity, for the annual indices (top) and June-only indices (bottom). The influence of the current GMST is shown with the red vs blue probability curves, showing the present (2026) vs past 1976 warming levels. The magnitude of the 1-in-X-year event is highlighted with a horizontal purple line, with X given for each variable and time period in Table 1.*

Variable		Change since preindustrial		Change since 1976		Change since 2003	
		Probability ratio	Change in magnitude (C)	Probability ratio	Change in magnitude (C)	Probability ratio	Change in magnitude (C)
WBGT	June	162 (4.01, inf)	3.03 (1.60, 4.50)	38.9 (3.00, inf)	2.38 (1.26, 3.53)	5.86 (1.83, inf)	1.30 (0.69, 1.93)
	Annual	Inf (9.90, inf)	3.02 (1.86, 4.10)	Inf (6.18, inf)	2.37 (1.46, 3.22)	96.7 (2.75, inf)	1.30 (0.80, 1.76)
Tx3x	June	263 (3.45, inf)	3.86 (1.99, 5.80)	49.7 (2.64, inf)	3.03 (1.56, 4.55)	6.26 (1.71, inf)	1.65 (0.85, 2.48)
	Annual	61.5 (4.62, inf)	4.21 (2.60, 5.53)	21.7 (3.36, inf)	3.30 (2.04, 4.35)	4.72 (1.97, 26.5)	1.80 (1.11, 2.37)
RH	June	0.75 (0.51, 1.02)	-5.29 (-10.4, +0.43)	0.79 (0.54, 1.02)	-4.16 (-8.15, +0.34)	0.86 (0.66, 1.01)	-2.27 (-4.45, +0.18)

	Annual	0.70 (0.51, 0.99)	-8.89 (-13.8, -0.31)	0.72 (0.53, 0.99)	-6.98 (-10.9, -0.25)	0.80 (0.62, 1.00)	-3.81 (-5.93, -0.13)

Table A1: *Estimated changes in likelihood and intensity for each variable - WBGT and the associated 3-day maximum temperatures (Tx3x) and relative humidity (RH) - associated with global warming since preindustrial conditions (approximately 1.4°C), 1976 (approximately 1.1°C), and 2003 (approximately 0.6°C).*

A2 Comparison of estimates of heat-related excess deaths using different methods

Table A2: *Comparison of heat-related deaths with previously reported estimates. We present estimates for summer 2003 as a benchmark for an extreme summer, alongside the heat episodes associated with the highest numbers of deaths in UKHSA reports since 2022, as well as heat periods for which estimates are available both from the methodological approach used in this report and from UKHSA, in order to facilitate comparison.*

Year	Event	Estimated heat-deaths	Average deaths per day	Source	Method
2003	4-13 August	2,139	N/A	Johnson et al	Excess wrt reference period
2022	10-25 July	1,256 (729 - 1,784)	79	UKHSA 2022	Excess wrt reference period
	17-19 July	1,064 (735 - 1,256)	355	Mistry et al	Parametric temperature-mortality curves
	8-17 August	1,633 (1,247 - 2,018)	102	UKHSA 2022	Excess wrt reference period
2023	3-13 September	934 (522 - 1,346)	85	UKHSA 2023	Excess wrt reference period
2024	18-20 July	467 (288 - 646)	156	UKHSA 2024	Excess wrt reference period
2025	19-22 June	570 (435 - 673)	143	Konstantinoudis et al	Parametric temperature-mortality curves
	19-22 June	253 (35 - 470)	63	UKHSA 2025	Excess wrt reference period
	10-16 August	697 (400 - 993)	100	UKHSA 2025	Excess wrt reference period
2026	21-29 May	553 (426 - 704)	61	current report	Parametric temperature-mortality curves
	18-28 June	2,183 (1,582 - 2,724)	198	current report	Parametric temperature-mortality curves

A3. Synthesis of monthly mean temperatures per county

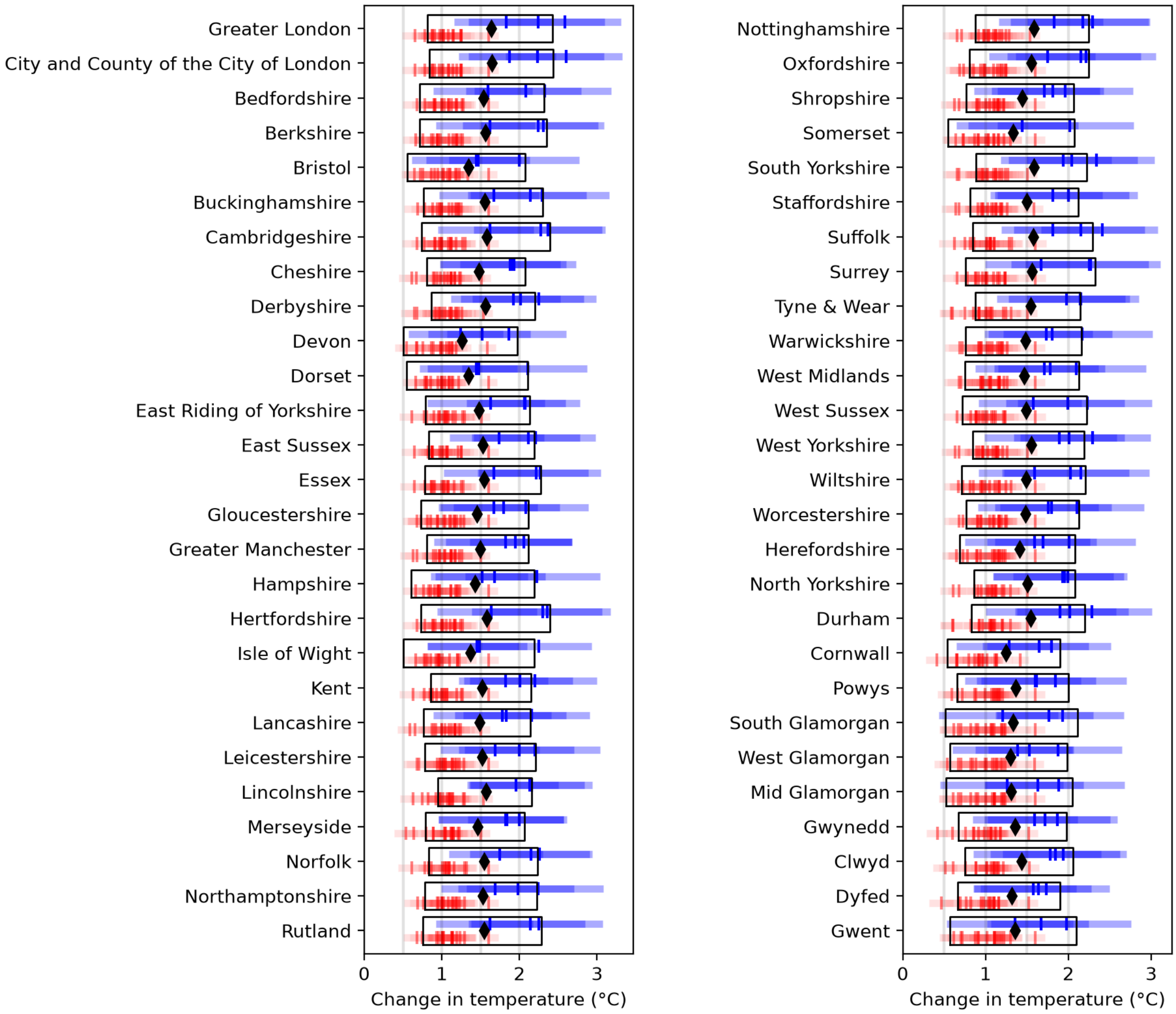

Figure A3: *Details of probabilistic attribution of change in mean May temperatures in each county. compared to a 1.4°C cooler climate without human-caused warming. Blue indicates estimated change in observations-based data products; red indicates change in climate models. Shaded bars represent bootstrapped uncertainties in each dataset; vertical ticks indicate results for individual datasets; black diamonds represent unweighted average of results from observations and models, with uncertainty represented by box.*

ACCESS-CM2 r1i1p1f1	*CMCC-CM2-SR5 r1i1p1f1*	***GFDL-CM4 r1i1p1f1***	*KIOST-ESM r1i1p1f1*
ACCESS-ESM1-5 r1i1p1f1	***CMCC-ESM2 r1i1p1f1***	***GFDL-ESM4 r1i1p1f1***	***MIROC-ES2L r1i1p1f2***

AWI-ESM-1-REcoM r1i1p1f1	*CNRM-CM6-1 r1i1p1f2*	*GISS-E2-1-G r1i1p1f2*	***MIROC6 r10i1p1f1***
BCC-CSM2-MR r1i1p1f1	*CNRM-CM6-1-HR r1i1p1f2*	***HadGEM3-GC31-LL r1i1p1f3***	***MPI-ESM1-2-LR r10i1p1f1***
CAMS-CSM1-0 r1i1p1f1	*CNRM-ESM2-1 r1i1p1f2*	*HadGEM3-GC31-MM r1i1p1f3*	***MRI-ESM2-0 r1i1p1f1***
CanESM5 r10i1p1f1	*E3SM-1-1 r1i1p1f1*	*IITM-ESM r1i1p1f1*	*NESM3 r1i1p1f1*
CanESM5-CanOE r1i1p2f1	*EC-Earth3-CC r1i1p1f1*	***INM-CM4-8 r1i1p1f1***	*NorESM2-LM r1i1p1f1*
CESM2 r10i1p1f1	***EC-Earth3-Veg-LR r1i1p1f1***	*INM-CM5-0 r1i1p1f1*	***NorESM2-MM r1i1p1f1***
CESM2-WACCM r1i1p1f1	*FGOALS-f3-L r1i1p1f1*	*IPSL-CM6A-LR r14i1p1f1*	***TaiESM1 r1i1p1f1***
CIESM r1i1p1f1	***FIO-ESM-2-0 r1i1p1f1***	*KACE-1-0-G r1i1p1f1*	***UKESM1-0-LL r1i1p1f2***

Table A2: *List of CMIP6 models used in the attribution analysis. Models highlighted in bold passed model evaluation (assessed on whether they correctly represented the shape and spread of monthly mean temperatures across more than 50% of counties) and were included in the final synthesised result.*

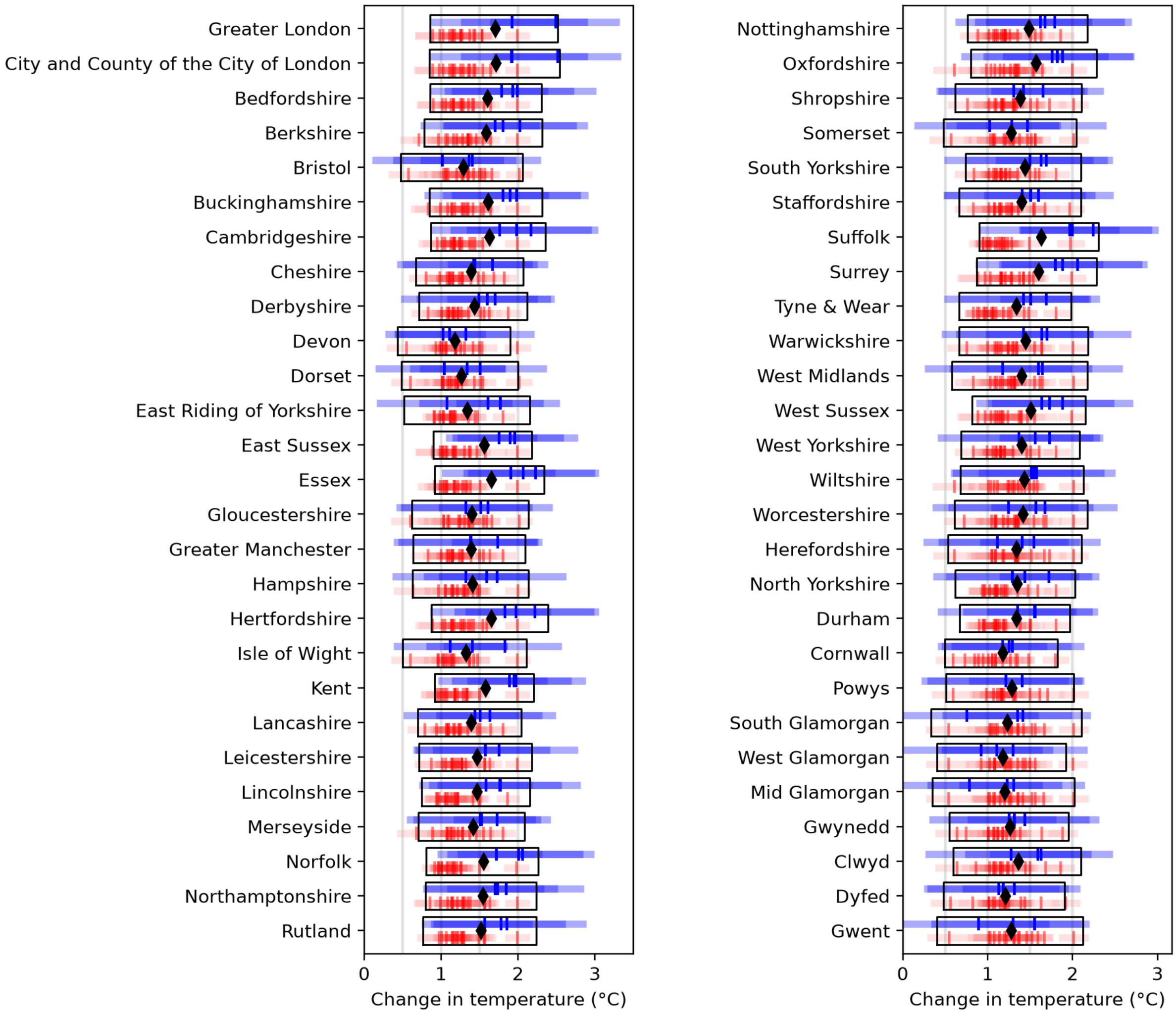

Figure A4: *As Figure A3, but for June.*